**This article is published as part of the *Dalton Transactions* themed issue entitled:**

# Contributions of Inorganic Chemistry to Energy Research

Guest Editors Duncan Wass and Neil Robertson
University of Bristol and University of Edinburgh, UK

Published in issue 15, 2011 of *Dalton Transactions*

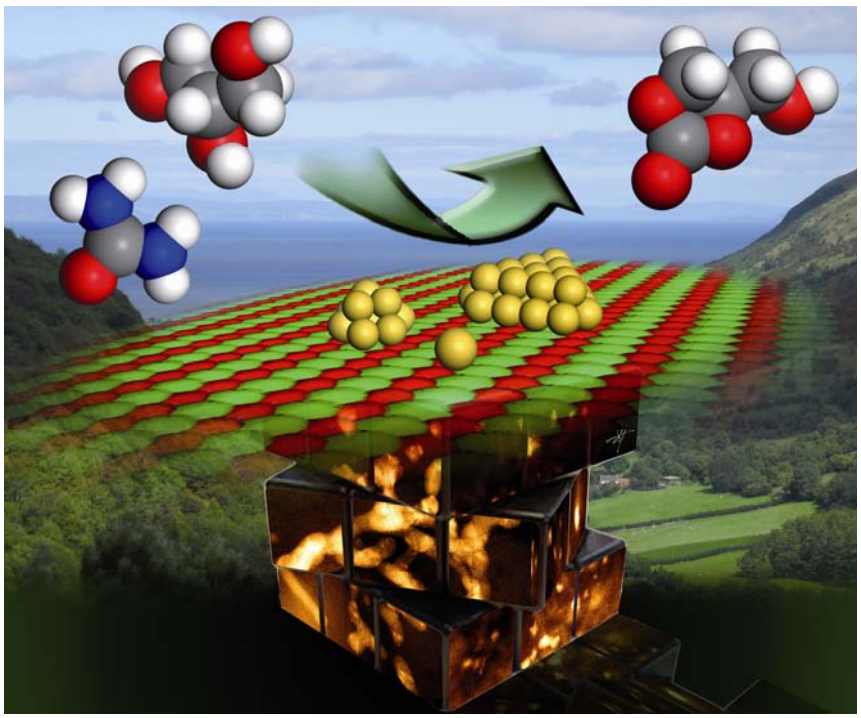

Image reproduced with permission of Graham Hutchings

*Articles in the issue include:*

**ARTICLES:**

# Surprising photochemical reactivity and visible light-driven energy transfer in heterodimetallic complexes†

**Sylvia Eller,[a] Barbara Trettenbrein,[a] Markus Fessler,[a] Stephan Haringer,[a] Martin Ruggenthaler,[a] Rene Gutmann,[a] Wytze E. van der Veer,[b] Holger Kopacka,[a] Thomas Müller,[c] Dagmar Obendorf[d] and Peter Brüggeller*[a]**

*Received 2nd April 2010, Accepted 16th October 2010*
**DOI: 10.1039/c0dt00253d**



The bis(bidentate) phosphine *cis*,*trans*,*cis*-1,2,3,4-tetrakis(diphenylphosphino)cyclobutane (dppcb) has been used for the synthesis of a series of novel heterodimetallic complexes starting from $[Ru(bpy)_2(dppcb)]X_2$ (**1**; X = $PF_6$, $SbF_6$), so-called dyads, showing surprising photochemical reactivity. They consist of $[Ru(bpy)_2]^{2+}$ "antenna" sites absorbing light combined with reactive square-planar metal centres. Thus, irradiating $[Ru(bpy)_2(dppcb)MCl_2]X_2$ (M = Pt, **2**; Pd, **3**; X = $PF_6$, $SbF_6$) dissolved in $CH_3CN$ with visible light, produces the unique heterodimetallic compounds $[Ru(bpy)(CH_3CN)_2(dppcb)MCl_2]X_2$ (M = Pt, **7**; Pd, **8**; X = $PF_6$, $SbF_6$). In an analogous reaction the separable diastereoisomers (ΔΛ/ΛΔ)- and (ΔΔ/ΛΛ)-$[Ru(bpy)_2(dppcb)Os(bpy)_2](PF_6)_4$ (**5/6**) lead to $[Ru(bpy)(CH_3CN)_2(dppcb)Os(bpy)_2](PF_6)_4$ (**9**), where only the $RuP_2N_4$ moiety of **5/6** is photochemically reactive. By contrast, in the case of $[Ru(bpy)_2(dppcb)NiCl_2]X_2$ (**4**; X = $PF_6$, $SbF_6$) no clean photoreaction is observed. Interestingly, this difference in photochemical behaviour is completely in line with the related photophysical parameters, where **2**, **3**, and **5/6**, but not **4**, show long-lived excited states at ambient temperature necessary for this type of photoreaction. Furthermore, the photochemical as well as the photophysical properties of **2–4** are also in accordance with their single crystal X-ray structures presented in this work. It seems likely that differences in "steric pressure" play a major role for these properties. The unique complexes **7–9** are also fully characterized by single-crystal X-ray structure analyses, clearly showing that the stretching vibration modes of the ligand $CH_3CN$, present only in **7–9**, cannot be directly influenced by "steric pressure". This has dramatic consequences for their photophysical parameters. The *trans*-$[Ru(bpy)(CH_3CN)_2]^{2+}$ chromophore of **9** acts as efficient "antenna" for visible light-driven energy transfer to the Os-centred "trap" site, resulting in $k_{en} \geq 2 \times 10^9$ $s^{-1}$ for the energy transfer. Since electron transfer is made possible by the use of this intervening energy transfer, in dyads like **2–4** highly reactive M(0) species (M = Pt, Pd, Ni) could be generated. These species are not stable in water and M(II) hydride intermediates are usually formed, further reacting with $H^+$ to give $H_2$. Thus, derivatives of **3**, namely $[M(bpy)_2(dppcb)Pd(bpy)](PF_6)_4$ (M = Os, Ru) dissolved in 1 : 1 (v/v) $H_2O$–$CH_3CN$ produce $H_2$ during photolysis with visible light.

## Introduction

It has been widely recognized that conversion of solar photons to electricity or fuels is an important task due to the risks of global climate change driven by society's reliance on carbonaceous energy resources.[1] Heterodimetallic transition metal complexes containing $[Ru(bpy)_2]^{2+}$ "antenna" sites absorb light efficiently over a wide spectral range, have long-lived excited states, and have multiple oxidation states.[2] Furthermore, heterodimetallic species consisting of these "Ru-bpy" chromophores together with additional transition metals like Pt(II), Pd(II) or Ni(II) are attractive for use as photocatalysts for fuels production.[2a] The metal-to-ligand charge-transfer (MLCT) excited-states of these $[Ru(bpy)_2]^{2+}$ moieties could be prone to oxidative quenching by Pt(II), Pd(II) or Ni(II), leading to highly reactive metal sites.[2a] Diphosphines stabilize these reactive species occurring upon redox switch during catalysis.[3] However, in the case of tetraphosphines only a few examples of heterodimetallic complexes containing the $[M(bpy)_2]^{2+}$ (M = Ru, Os) chromophores are known.[2b,4]

In this work the first examples of photochemically reactive $[Ru(bpy)_2]^{2+}$ moieties combined with bis(bidentate) phosphine-connected reactive square-planar metal centres are presented.[2b,5] The bis(bidentate) tetraphosphine *cis*,*trans*,*cis*-1,2,3,4-tetrakis(diphenylphosphino)cyclobutane (dppcb), that has been carefully designed in our laboratory in order to make dimetallic species possible,[6] leads to "steric pressure" in sterically demanding dimetallic complexes.[2b,5,7] Proof positive has been presented that this "steric pressure" produces long-lived excited

[a]*Institute of General, Inorganic and Theoretical Chemistry, University of Innsbruck, Innrain 52a, 6020, Innsbruck, Austria. E-mail: Peter.Brueggeller@uibk.ac.at; Fax: +43 512 507 2934; Tel: +43 512 507 5115*
[b]*Department of Chemistry, University of California, Irvine, CA, 92697-2025, USA*
[c]*Institute of Organic Chemistry, University of Innsbruck, Innrain 52a, 6020, Innsbruck, Austria*
[d]*Institute of Analytical Chemistry and Radiochemistry, University of Innsbruck, Innrain 52a, 6020, Innsbruck, Austria*

† Electronic supplementary information (ESI) available: Details of the photophysical and electrochemical measurements. CCDC reference numbers 772256–772261. For ESI and crystallographic data in CIF or other electronic format see DOI: 10.1039/c0dt00253d

states even for $RuP_2N_4$ type chromophores at ambient temperature and as a consequence photochemical reactivity.[2b,5] Surprisingly, also the new heterodimetallic species $[Ru(bpy)_2(dppcb)MCl_2]X_2$ (M = Pt, **2**; Pd, **3**; X = $PF_6$, $SbF_6$) are photochemically reactive, where the "steric pressure" is clearly reduced due to the presence of sterically less demanding square-planar metal centres (see Scheme 1).[2b,5,7] However, in the case of $[Ru(bpy)_2(dppcb)NiCl_2]X_2$ (**4**; X = $PF_6$, $SbF_6$) the reduction of the square-planar stabilization energy of nickel(II) compared with platinum(II) and palladium(II)[8] makes **4** flexible enough to enhance the non-radiative decay of its excited states.[2b,5] As a consequence for **4** neither a long-lived excited state at ambient temperature can be observed nor a photochemical product can be isolated.

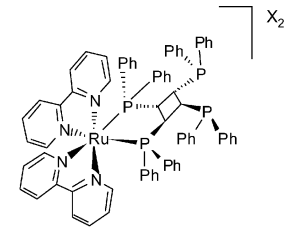

$[Ru(bpy)_2(dppcb)]X_2$ (**1**)
X = $PF_6$, $SbF_6$

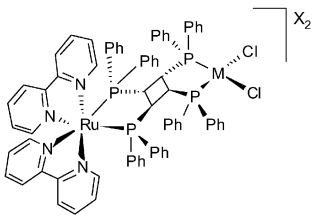

$[Ru(bpy)_2(dppcb)MCl_2]X_2$
X = $PF_6$, $SbF_6$
M = Pt (**2**)
M = Pd (**3**)
M = Ni (**4**)

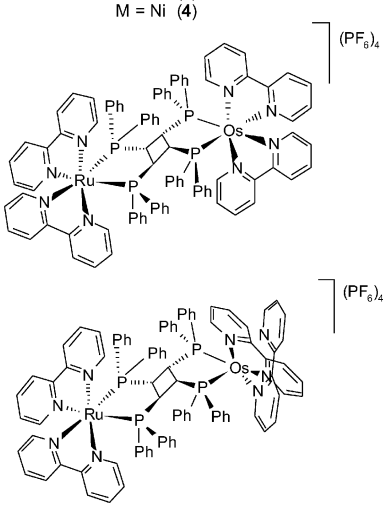

(ΔΛ/ΛΔ)- and (ΔΔ/ΛΛ)-
$[Ru(bpy)_2(dppcb)Os(bpy)_2](PF_6)_4$ (**5/6**)

**Scheme 1**

The novel heterodimetallic compounds **2–4** as well as the separable diastereoisomers (ΔΛ/ΛΔ)- and (ΔΔ/ΛΛ)-$[Ru(bpy)_2(dppcb)Os(bpy)_2](PF_6)_4$ (**5/6**) have been prepared starting from the precursor complex $[Ru(bpy)_2(dppcb)]X_2$ (**1**; X = $PF_6$, $SbF_6$; see Scheme 1). **1** is obtainable *via* a suitable entropy effect using an excess of dppcb.[4b] Clearly, **5/6** should be regarded as supramolecular complexes,[1c,d,9] since fast energy transfer with $k_{en} \geq 2 \times 10^9$ $s^{-1}$ occurs from the $[Ru(bpy)_2]^{2+}$ "antenna" site to the $[Os(bpy)_2]^{2+}$ "trap" site.[2b] The velocity of this energy transfer corresponds to the Dexter (exchange) mechanism, indicating through-space overlap of the wavefunctions of the $Ru^{II}$ energy donor and the $Os^{II}$ energy acceptor, since in heterodimetallic species containing dppcb a region of saturated carbons disrupts significant electronic wave function mixing through the cyclobutane backbone "bridge".[2b,10] This means that also coupling of light absorption to electron transfer becomes possible in the heterodimetallic compounds **2–6**. There are relatively few reports on homogeneous catalysts for the light-driven hydrogen production by water splitting.[11] In this context the photogenerated reduction of the reactive $Pt^{II}$, $Pd^{II}$ or $Ni^{II}$ sites in **2–4** and analogous complexes could be a very interesting photophysical reactivity.

Furthermore, irradiating **2**, **3** or **5/6** in $CH_3CN$ with visible light leads to the unique heterodimetallic species $[Ru(bpy)(CH_3CN)_2(dppcb)MCl_2]X_2$ (M = Pt, **7**; Pd, **8**; X = $PF_6$, $SbF_6$) and $[Ru(bpy)(CH_3CN)_2(dppcb)Os(bpy)_2](PF_6)_4$ (**9**; see Scheme 2), respectively. This extraordinary photochemical reactivity is strongly connected with the special steric properties of dppcb, since $[Ru(bpy)_2]^{2+}$ chromophores combined with simple mono- or diphosphines show no photochemistry at all.[5b,12] This behaviour is comparable to $[Ru(bpy)_3]^{2+}$, being well-known for its light stability.[13] Complications remain from low-lying, metal-centred d → d excited states.[14] They are typically populated by thermally activated barrier crossing following MLCT excitation.

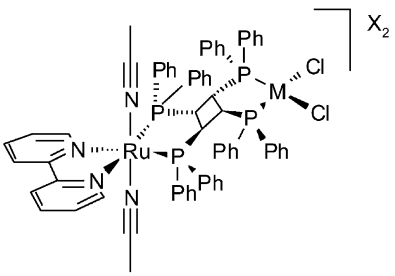

$[Ru(bpy)(CH_3CN)_2(dppcb)MCl_2]X_2$
X = $PF_6$, $SbF_6$
M = Pt (**7**)
M = Pd (**8**)

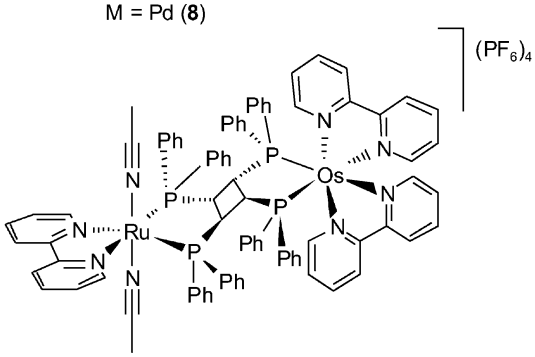

$[Ru(bpy)(CH_3CN)_2(dppcb)Os(bpy)_2](PF_6)_4$ (**9**)

**Scheme 2**

 

Their population leads to shortened lifetimes and net ligand-loss photochemistry.[14] The activation energies for this thermal activation calculated from Arrhenius-plots for **2** and **3** in this work clearly explain their clean photochemical reactivity. Dynamic molecular systems in which a given part of a molecular system can be set in motion at will under the action of an external signal are often referred to as molecular machines or motors.[15] Thus, photochemical ligand exchange has rather been considered a detrimental reaction only until now,[15a] since it could induce an interesting photophysical reactivity.

## Experimental

### Reagents and general procedures

Dppcb was prepared as described earlier.[6] *cis*-$[OsCl_2(bpy)_2]$, *cis*-$[RuCl_2(bpy)_2]\cdot 2H_2O$, $[MCl_2(\eta^4\text{-COD})]$ (M = Pt, Pd), $[NiCl_2(DME)]$, $NH_4PF_6$, $NaPF_6$, and $NaSbF_6$ were obtained commercially. Dry solvents of purissimum grade were used for all syntheses, spectroscopic measurements, and crystallization purposes. A Schlenk apparatus and oxygen-free, dry Ar were utilized in the syntheses of all complexes. Solvents were degassed by several freeze–pump–thaw cycles prior to use.

### Instrumentation

Fourier-mode $^{195}Pt\{^1H\}$, $^{31}P\{^1H\}$, $^{13}C\{^1H\}$, and $^1H$ NMR spectra were obtained using a Bruker DPX-300 spectrometer (internal deuterium lock), unless stated otherwise. Positive chemical shifts are downfield from the standards: 1.0 M $Na_2PtCl_6$ for the $^{195}Pt\{^1H\}$, 85% $H_3PO_4$ for the $^{31}P\{^1H\}$, and TMS for the $^{13}C\{^1H\}$ and $^1H$ resonances. The NMR parameters are given at ambient temperature, unless stated otherwise. Within the compounds **1–9**, the $^{13}C\{^1H\}$ NMR spectra in $CD_3CN$ are rather insensitive to structural variations. The $^{13}C\{^1H\}$ NMR resonances of the 2,2′-bipyridine and phenyl rings occur in the ranges 145–160 and 135–145, respectively, as broad multiplets. However, the $^{13}C\{^1H\}$ NMR signals of the cyclobutane rings are only occasionally observable at about 45 and no further signals can be detected due to the restricted solubility of these complexes. For the compounds **7–9** containing $CH_3CN$ ligands, the ν(CN) vibrations in the IR spectra (KBr) are obscured by lattice vibrations of dppcb. FAB- and ESI-MS spectra were obtained on a Finnigan MAT-95 spectrometer, using 3-nitrobenzylalcohol (NOBA) as matrix. Elemental analyses were performed using a Perkin Elmer Model 2400 C,H,N elemental analyser. The details of the photophysical and electrochemical measurements are given as ESI.†

### Syntheses

**$[Ru(bpy)_2(dppcb)]X_2$ (1; X = $PF_6$, $SbF_6$).** In a three-neck flask dppcb (0.6000 g, 0.757 mmol) was boiled in THF (60 mL). *cis*-$[RuCl_2(bpy)_2]\cdot 2H_2O$ (0.1311 g, 0.252 mmol) dissolved in ethylene glycol (50 mL) was added dropwise *via* a dropping funnel over 3 h with vigorous stirring. Afterwards the solution was stirred under reflux for 4 h. Then an excess of $NH_4PF_6$ (0.4110 g, 2.52 mmol) was added and the reaction mixture was stirred under reflux for another 72 h. The slurry was cooled to room temperature, THF was removed by means of a vacuum pump and a saturated $NaPF_6$-solution in water (200 mL) was slowly added. A light yellow powder was filtered off, washed with water and dried *in vacuo*. In order to remove the excess of the ligand dppcb quantitatively, the powder was washed three times with toluene and the yellow residue was dried *in vacuo*. (Yield: 0.3620 g, 96.0%.) The ligand dppcb can be recycled from the toluene solution *via* removing the toluene completely by means of a vacuum pump. The complete characterization of **1** including its single-crystal X-ray structure analysis has already been reported elsewhere in a preliminary communication.[5a] $[Ru(bpy)_2(dppcb)](SbF_6)_2$ has been prepared in an analogous manner using $NaSbF_6$.

**$[Ru(bpy)_2(dppcb)PtCl_2]X_2$ (2; X = $PF_6$, $SbF_6$).** $[Ru(bpy)_2(dppcb)](PF_6)_2$ (**1**; 0.0700 g, 0.0468 mmol) was dissolved in $CH_2Cl_2$ (20 mL) and $[PtCl_2(\eta^4\text{-COD})]$ (0.0175 g, 0.0468 mmol) was added in solid form with vigorous stirring. After 15 min a yellow precipitate formed. The yellow residue was filtered off, washed with $CH_2Cl_2$ and dried *in vacuo*. A yellow micro-crystalline powder was recrystallized from 1 : 1 (v/v) $CH_2Cl_2$–$CH_3CN$ and then dried under vacuum. (Yield: 0.0625 g, 75.8%.) Mp = 303 °C dec. (Found: C 48.99, H 3.52, N 3.07, $C_{72}H_{60}Cl_2F_{12}N_4P_6PtRu$ (1762.166) requires C 49.08, H 3.43, N 3.18%.) $^{195}Pt\{^1H\}$ NMR ($CD_3CN$): $\delta$ –4520 (dd). $^{31}P\{^1H\}$ NMR ($CH_3CN$): $\delta$ 85.7 (dd, $^2J(P,P) + {}^3J(P,P)_{cis}$ = 10.4 Hz, $^3J(P,P)_{trans}$ = 12.0 Hz, $P_{Ru}$), 83.7 (dt, $^2J(P,P) + {}^3J(P,P)_{cis} = {}^3J(P,P)_{trans}$ = 10.4 Hz, $^4J(P,P)_{trans}$ = 5.9 Hz, $P_{Ru}$), 54.5 (dd, $^2J(P,P) + {}^3J(P,P)_{cis}$ = 12.0 Hz, $^3J(P,P)_{trans}$ = 10.4 Hz, $^1J(Pt,P)$ = 3652 Hz, $P_{Pt}$), 52.7 (dt, $^2J(P,P) + {}^3J(P,P)_{cis} = {}^3J(P,P)_{trans}$ = 12.0 Hz, $^4J(P,P)_{trans}$ = 5.9 Hz, $^1J(Pt,P)$ = 3659 Hz, $P_{Pt}$), –142.7 (septet, $^1J(P,F)$ = 709 Hz, $PF_6^-$). $^1H$ NMR ($CD_3CN$): $\delta$ 9.40 (d, $^3J(H, H)$ = 5.3 Hz, 2 H, bpy-*H*), 8.45 (t, $^3J(H, H)$ = 7.4 Hz, 2 H, bpy-*H*), 8.40 (t, $^3J(H, H)$ = 8.3 Hz, 2 H, bpy-*H*), 8.20 (d, $^3J(H, H)$ = 8.3 Hz, 2 H, bpy-*H*), 8.00 (t, $^3J(H, H)$ = 8.0 Hz, 2 H, bpy-*H*), 7.88 (t, $^3J(H, H)$ = 6.6 Hz, 2 H, bpy-*H*), 7.80 (d, $^3J(H, H)$ = 5.2 Hz, 2 H, bpy-*H*), 7.67 (d, $^3J(H, H)$ = 5.3 Hz, 2 H, bpy-*H*), 5.60–7.60 (m, 40 H, phenyl-*H*), 4.18 (br m, 2 H, C*H*), 3.97 (br m, 2 H, C*H*). Positive ion ESI-MS: $m/z$ ($m/z_{calcd}$) 1617.5 (1617.2) $[M - PF_6]^+$. UV-vis absorption: $\lambda_{max}$ ($4.0 \times 10^{-4}$ M in $CH_3CN$)/nm 271 ($\varepsilon$/dm$^3$ mol$^{-1}$ cm$^{-1}$ 34 000), 303 (22 000), 323 (13 000) and 377 (6800). $E_{1/2}$ values *vs.* SCE ($\Delta E$, $\Delta E_p$ [mV]): $Pt^{II/IV}$ +1.27 V [irr.], $Ru^{II/III}$ +1.16 V [70], $Pt^{II/0}$ –0.33 V [irr.], first $bpy^{0/-}$ –1.85 V [70], second $bpy^{0/-}$ –2.14 V [80]. Single crystals suitable for an X-ray structure analysis with the composition $[Ru(bpy)_2(dppcb)PtCl_2](PF_6)_2\cdot 3.5CH_2Cl_2\cdot 0.5H_2O$ were obtained by gas-phase diffusion of *n*-hexane into a $CH_2Cl_2$ solution of $[Ru(bpy)_2(dppcb)PtCl_2](PF_6)_2$ (**2**) at room temperature. This crystallization was only successful under an atmosphere of air, since water molecules are incorporated into the crystal lattice. $[Ru(bpy)_2(dppcb)PtCl_2](SbF_6)_2$ has been prepared in an analogous manner starting from $[Ru(bpy)_2(dppcb)](SbF_6)_2$.

**$[Ru(bpy)_2(dppcb)PdCl_2]X_2$ (3; X = $PF_6$, $SbF_6$).** To a solution of $[Ru(bpy)_2(dppcb)](PF_6)_2$ (**1**; 0.0700 g, 0.0468 mmol) in $CH_2Cl_2$ (20 mL), $[PdCl_2(\eta^4\text{-COD})]$ (0.0134 g, 0.0468 mmol) was added in solid form with vigorous stirring. A yellow precipitate formed and the suspension was stirred at ambient temperature for 12 h. Then a yellow powder was filtered off, washed with $CH_2Cl_2$ and dried *in vacuo*. A yellow micro-crystalline powder was recrystallized from 1 : 1 (v/v) $CH_2Cl_2$–$CH_3CN$ and then dried under vacuum. (Yield: 0.0502 g, 64.1%.) Mp = 314 °C. (Found: C 51.52, H 3.70, N 3.30, $C_{72}H_{60}Cl_2F_{12}N_4P_6PdRu$ (1673.506) requires C 51.68, H

3.61, N 3.35%.) $^{31}P\{^{1}H\}$ NMR ($CH_3CN$): $\delta$ 86.3 (dd, $^{2}J(P,P) + {}^{3}J(P,P)_{cis} = 11.0$ Hz, $^{3}J(P,P)_{trans} = 13.0$ Hz, $P_{Ru}$), 85.6 (dt, $^{2}J(P,P) + {}^{3}J(P,P)_{cis} = {}^{3}J(P,P)_{trans} = 11.0$ Hz, $^{4}J(P,P)_{trans} = 7.0$ Hz, $P_{Ru}$), 76.1 (ddd, $^{2}J(P,P) + {}^{3}J(P,P)_{cis} = 11.0$ Hz, $^{3}J(P,P)_{trans} = 13.0$ Hz, $^{4}J(P,P)_{trans} = 7.0$ Hz, $P_{Pd}$), 75.3 (t, $^{2}J(P,P) + {}^{3}J(P,P)_{cis} = {}^{3}J(P,P)_{trans} = 11.0$ Hz, $P_{Pd}$), −143.6 (septet, $^{1}J(P,F) = 707$ Hz, $PF_6^-$). $^{1}H$ NMR ($CD_3CN$): $\delta$ 9.35 (d, $^{3}J(H, H) = 2.0$ Hz, 2 H, bpy-*H*), 8.42 (m, 2 H, bpy-*H*), 8.22 (d, $^{3}J(H, H) = 2.0$ Hz, 2 H, bpy-*H*), 8.07 (m, 2 H, bpy-*H*), 7.78 (m, 8 H, bpy-*H*), 5.66–7.65 (br m, 40 H, phenyl-*H*), 5.45 (br m, 1 H, C*H*), 4.00 (br m, 1 H, C*H*), 3.47 (br m, 1 H, C*H*), 2.76 (br m, 1 H, C*H*). Positive ion ESI-MS: $m/z$ ($m/z_{calcd}$) 1528.5 (1528.5) $[M - PF_6]^+$, 691.8 (691.8) $[M - 2PF_6]^{2+}$. UV-vis absorption: $\lambda_{max}$ ($4.0 \times 10^{-4}$ M in $CH_3CN$)/nm 269 ($\varepsilon$/dm$^3$ mol$^{-1}$ cm$^{-1}$ 37 000), 293 (21 000), 324 (15 000) and 375 (7400). $E_{1/2}$ values *vs.* SCE ($\Delta E$, $\Delta E_p$ [mV]): $Pd^{II/IV}$ +1.50 V [irr.], $Ru^{II/III}$ +1.10 V [shoulder], $Pd^{II/0}$ −0.14 V [irr.], first $bpy^{0/-}$ −1.21 V [80], second $bpy^{0/-}$ −1.45 V [80]. Single crystals suitable for an X-ray structure analysis with the composition $[Ru(bpy)_2(dppcb)PdCl_2](PF_6)_2 \cdot 1.3CH_2Cl_2 \cdot H_2O$ were obtained by gas-phase diffusion of *n*-hexane into a $CH_2Cl_2$ solution of $[Ru(bpy)_2(dppcb)PdCl_2](PF_6)_2$ (**3**) at room temperature. This crystallization was only successful under an atmosphere of air, since water molecules are incorporated into the crystal lattice. $[Ru(bpy)_2(dppcb)PdCl_2](SbF_6)_2$ has been prepared in an analogous manner starting from $[Ru(bpy)_2(dppcb)](SbF_6)_2$.

**$[Ru(bpy)_2(dppcb)NiCl_2]X_2$ (4; X = $PF_6$, $SbF_6$).** $[Ru(bpy)_2(dppcb)](PF_6)_2$ (**1**; 0.0700 g, 0.0468 mmol) was dissolved in $CH_2Cl_2$ (20 mL) and $[NiCl_2(DME)]$ (0.0103 g, 0.0468 mmol) was added in solid form with vigorous stirring. After 12 h of reaction time at ambient temperature an orange precipitate was filtered off, washed with $CH_2Cl_2$ and dried *in vacuo*. The residue was recrystallized from 1 : 1 (v/v) $CH_2Cl_2$–$CH_3CN$, the produced red crystals were collected and then dried under vacuum. (Yield: 0.0441 g, 58.0%.) Mp = 268 °C. (Found: C 47.64, H 3.86, N 2.87, $C_{75.7}H_{71.4}Cl_{7.4}F_{12}N_4NiO_2P_6Ru$ (1905.077) requires C 47.73, H 3.78, N 2.94%.) $^{31}P\{^{1}H\}$ NMR (238 K, $CH_3CN$): $\delta$ 86.3 (t, $^{2}J(P,P) + {}^{3}J(P,P)_{cis} = {}^{3}J(P,P)_{trans} = 11.0$ Hz, $P_{Ru}$), 84.8 (t, $^{2}J(P,P) + {}^{3}J(P,P)_{cis} = {}^{3}J(P,P)_{trans} = 11.0$ Hz, $P_{Ru}$), 68.7 (dd, $^{2}J(P,P) + {}^{3}J(P,P)_{cis} = 64.0$ Hz, $^{3}J(P,P)_{trans} = 11.0$ Hz, $P_{Ni}$), 66.2 (dd, $^{2}J(P,P) + {}^{3}J(P,P)_{cis} = 64.0$ Hz, $^{3}J(P,P)_{trans} = 11.0$ Hz, $P_{Ni}$), −143.4 (septet, $^{1}J(P,F) = 706$ Hz, $PF_6^-$). $^{1}H$ NMR ($CD_3CN$): $\delta$ 9.31 (d, $^{3}J(H, H) = 5.0$ Hz, 2 H, bpy-*H*), 8.46 (d, $^{3}J(H, H) = 7.0$ Hz, 2 H, bpy-*H*), 8.40 (t, $^{3}J(H, H) = 7.0$ Hz, 2 H, bpy-*H*), 8.22 (d, $^{3}J(H, H) = 8.0$ Hz, 2 H, bpy-*H*), 8.13 (br s, 2 H, bpy-*H*), 8.06 (t, $^{3}J(H, H) = 8.0$ Hz, 2 H, bpy-*H*), 7.75 (m, 4 H, bpy-*H*), 6.33–7.65 (br m, 40 H, phenyl-*H*), 5.30 (br m, 1 H, C*H*), 4.00 (br m, 1 H, C*H*), 3.17 (br m, 1 H, C*H*), 2.36 (br m, 1 H, C*H*). Positive ion ESI-MS: $m/z$ ($m/z_{calcd}$) 1480.6 (1480.8) $[M - PF_6]^+$, 667.9 (667.9) $[M - 2PF_6]^{2+}$, 602.9 (603.1) $[M - 2PF_6 - NiCl_2]^{2+}$. UV-vis absorption: $\lambda_{max}$ ($4.0 \times 10^{-4}$ M in $CH_3CN$)/nm 277 ($\varepsilon$/dm$^3$ mol$^{-1}$ cm$^{-1}$ 24 000), 324 (8900), 378 (5700) and 475 (1200). $E_{1/2}$ values *vs.* SCE ($\Delta E$, $\Delta E_p$ [mV]): $Ru^{II/III}$ +1.10 V [80], $Ni^{II/III}$ +0.74 V [irr.], first $bpy^{0/-}$ −1.13 V [80], second $bpy^{0/-}$ −1.44 V [90]. Single crystals suitable for an X-ray structure analysis with the composition $[Ru(bpy)_2(dppcb)NiCl_2](PF_6)_2 \cdot 2.7CH_2Cl_2 \cdot H_2O \cdot MeOH$ were obtained by slow evaporation of a 1 : 1 : 1 (v/v) $CH_2Cl_2$–$CH_3CN$–MeOH solution of $[Ru(bpy)_2(dppcb)NiCl_2](PF_6)_2$ (**4**) at ambient temperature. This crystallization was only successful under an atmosphere of air, since water molecules are incorporated into the crystal lattice. $[Ru(bpy)_2(dppcb)NiCl_2](SbF_6)_2$ has been prepared in an analogous manner starting from $[Ru(bpy)_2(dppcb)](SbF_6)_2$.

**(ΔΛ/ΛΔ)- and (ΔΔ/ΛΛ)-$[Ru(bpy)_2(dppcb)Os(bpy)_2](PF_6)_4$ (5/6).** A solution of *cis*-$[OsCl_2(bpy)_2]$ (0.0500 g, 0.0872 mmol) in ethylene glycol (40 mL) was heated up to 110 °C and $[Ru(bpy)_2(dppcb)](PF_6)_2$ (**1**; 0.1305 g, 0.0872 mmol) dissolved in $CH_3CN$ (40 mL) was added dropwise *via* a dropping funnel with vigorous stirring. The solution was stirred for 60 h. Then an excess of $NH_4PF_6$ (0.4000 g, 2.45 mmol) was added and the solution was stirred for another 48 h. After cooling the solution down to room temperature a saturated solution of $NaPF_6$ in water (100 mL) was added. A light orange precipitate formed, was filtered off, washed with water and dried *in vacuo*. The residue was washed three times with $CH_2Cl_2$ and then dried under vacuum. (Yield: 0.1118 g, 56.0%.) The complete characterization of **5/6** including the separation of the diastereoisomers by partial crystallization and the single-crystal X-ray structure analysis of (ΔΛ/ΛΔ)-$[Ru(bpy)_2(dppcb)Os(bpy)_2](PF_6)_4$ (**5**) has already been reported elsewhere in a preliminary communication.[2b]

**$[Ru(bpy)(CH_3CN)_2(dppcb)PtCl_2]X_2$ (7; X = $PF_6$, $SbF_6$).** $[Ru(bpy)_2(dppcb)PtCl_2](PF_6)_2$ (**2**; 0.0300 g, 0.0170 mmol) was dissolved in $CH_3CN$ (20 mL) and this solution was irradiated with an un-focused 700 W medium pressure Hg lamp with vigorous stirring for 42 h. The solvent was completely removed, the residue was suspended in $CH_2Cl_2$ (20 mL) and stirred for 72 h. A yellowish powder was filtered off, washed with $CH_2Cl_2$ and dried *in vacuo*. (Yield: 0.0158 g, 55.0%.) Mp = 125 °C. (Found: C 46.83, H 3.57, N 3.20, $C_{66}H_{58}Cl_2F_{12}N_4P_6PtRu$ (1688.085) requires C 46.96, H 3.46, N 3.32%.) $^{195}Pt\{^{1}H\}$ NMR ($CD_3CN$): $\delta$ −4524 (t). $^{31}P\{^{1}H\}$ NMR ($CH_3CN$): $\delta$ 79.3 (t, $^{2}J(P,P) + {}^{3}J(P,P)_{cis} = {}^{3}J(P,P)_{trans} = 12.0$ Hz, $2P_{Ru}$), 58.3 (t, $^{2}J(P,P) + {}^{3}J(P,P)_{cis} = {}^{3}J(P,P)_{trans} = 12.0$ Hz, $^{1}J(Pt,P) = 3618$ Hz, $2P_{Pt}$), −143.2 (septet, $^{1}J(P,F) = 698$ Hz, $PF_6^-$). $^{1}H$ NMR ($CD_3CN$): $\delta$ 8.53 (d, $^{3}J(H, H) = 8.1$ Hz, 2 H, bpy-*H*), 8.43 (br s, 2 H, bpy-*H*), 8.21 (t, $^{3}J(H, H) = 12.0$ Hz, 2 H, bpy-*H*), 7.54 (t, $^{3}J(H, H) = 6.6$ Hz, 2 H, bpy-*H*), 6.50–7.40 (br m, 40 H, phenyl-*H*), 4.88 (m, 2 H, $CH_{Ru\text{-}site}$), 3.64 (m, 2 H, $CH_{Pt\text{-}site}$), 2.18 (s, 3 H, $CH_3CN$), 0.86 (s, 3 H, $CH_3CN$). The assignment of the cyclobutane ring hydrogen atoms was carried out *via* a $^{31}P$–$^{1}H$ 2D NMR coupling experiment, where only in the case of **7** the solubility was high enough for this kind of assignment. Positive ion FAB-MS: $m/z$ ($m/z_{calcd}$) 1543.0 (1543.1) $[M - PF_6]^+$, 1357.1 (1357.1) $[M - 2PF_6 - CH_3CN]^+$, 1316.0 (1316.1) $[M - 2PF_6 - 2CH_3CN]^+$. UV-vis absorption: $\lambda_{max}$ ($2.7 \times 10^{-5}$ M in $CH_3CN$)/nm 233 ($\varepsilon$/dm$^3$ mol$^{-1}$ cm$^{-1}$ 49 000), 270 (17 000), 318 (9100) and 347 (3300). Single crystals suitable for an X-ray structure analysis with the composition $[Ru(bpy)(CH_3CN)_2(dppcb)PtCl_2](SbF_6)_2$ were obtained by slow evaporation of a $CH_3CN$ solution of $[Ru(bpy)(CH_3CN)_2(dppcb)PtCl_2](SbF_6)_2$ (**7**) under an Ar atmosphere at ambient temperature. In this case the choice of $SbF_6^-$ anions was essential in order to obtain good quality single crystals. $[Ru(bpy)(CH_3CN)_2(dppcb)PtCl_2](SbF_6)_2$ has been prepared in an analogous manner starting from $[Ru(bpy)_2(dppcb)PtCl_2](SbF_6)_2$.

**$[Ru(bpy)(CH_3CN)_2(dppcb)PdCl_2]X_2$ (8; X = $PF_6$, $SbF_6$).** Procedure as per that of $[Ru(bpy)(CH_3CN)_2(dppcb)PtCl_2](PF_6)_2$ (**7**), where $[Ru(bpy)_2(dppcb)PdCl_2](PF_6)_2$ (**3**; 0.0300 g, 0.0179 mmol) was used. (Yield: 0.0103 g, 36.0%.) Mp = 210 °C dec. (Found: C 49.41, H 3.73, N 3.37, $C_{66}H_{58}Cl_2F_{12}N_4P_6PdRu$ (1599.425) requires

 

**Table 1** Crystallographic data for $[Ru(bpy)_2(dppcb)MCl_2](PF_6)_2$ (M = Pt, **2**; Pd, **3**; Ni, **4**)

| Compound | **2** | **3** | **4** |
|---|---|---|---|
| Chemical formula | $C_{72}H_{60}Cl_2F_{12}N_4P_6PtRu\cdot 3.5CH_2Cl_2\cdot 0.5H_2O$ | $C_{72}H_{60}Cl_2F_{12}N_4P_6PdRu\cdot 1.3CH_2Cl_2\cdot H_2O$ | $C_{72}H_{60}Cl_2F_{12}N_4NiP_6Ru\cdot 2.7CH_2Cl_2\cdot H_2O\cdot MeOH$ |
| Formula weight | 2065.34 | 1801.25 | 1899.03 |
| Crystal system | Monoclinic | Monoclinic | Monoclinic |
| Space group | *P*2/*c* | *P*2/*c* | *Cc* |
| *a*/Å | 25.4693(8) | 25.2396(5) | 21.7459(4) |
| *b*/Å | 13.6167(5) | 13.4989(3) | 15.6939(3) |
| *c*/Å | 25.9759(9) | 25.5113(6) | 24.8759(3) |
| *β*/° | 117.403(2) | 118.250(1) | 91.379(1) |
| *U*/Å$^3$ | 7997.8(5) | 7656.6(3) | 8487.1(2) |
| *T*/K | 213 | 243 | 223 |
| *Z* | 4 | 4 | 4 |
| Measured reflections | 24 187 | 28 466 | 24 545 |
| Independent reflections | 14 011 ($R_{int}$ = 0.0390) | 14 901 ($R_{int}$ = 0.0337) | 19 492 ($R_{int}$ = 0.0263) |
| Final $R_1$, w$R_2$ [$I > 2\sigma(I)$ **2**; $I > 3\sigma(I)$ **3**, **4**] | 0.0497, 0.1522 | 0.0486, 0.1317 | 0.0400, 0.1145 |

C 49.56, H 3.65, N 3.50%.) $^{31}P\{^1H\}$ NMR ($CH_3CN$): $\delta$ 80.7 (t, $^2J(P,P) + {}^3J(P,P)_{cis} = {}^3J(P,P)_{trans}$ = 12.0 Hz, $2P_{Ru}$), 79.0 (t, $^2J(P,P) + {}^3J(P,P)_{cis} = {}^3J(P,P)_{trans}$ = 12.0 Hz, $2P_{Pd}$), −143.2 (septet, $^1J(P,F)$ = 710 Hz, $PF_6^-$). $^1H$ NMR ($CD_3CN$, 500 MHz): $\delta$ 8.58 (d, $^3J(H, H)$ = 5.0 Hz, 2 H, bpy-*H*), 8.45 (br s, 2 H, bpy-*H*), 8.24 (t, $^3J(H, H)$ = 4.0 Hz, 2 H, bpy-*H*), 7.56 (t, $^3J(H, H)$ = 4.0 Hz, 2 H, bpy-*H*), 7.25–7.51 (br m, 40 H, phenyl-*H*), 5.02 (br m, 2 H, C*H*), 3.92 (br m, 2 H, C*H*), 2.35 (s, 3 H, C*H*$_3$CN), 0.93 (s, 3 H, C*H*$_3$CN). Positive ion FAB-MS: *m*/*z* (*m*/*z*$_{calcd}$) 1455.2 (1455.5) $[M + H - PF_6]^+$, 1267.1 (1267.4) $[M - H - 2PF_6 - CH_3CN]^+$. UV-vis absorption: $\lambda_{max}$ ($2.4 \times 10^{-5}$ M in $CH_3CN$)/nm 233 ($\varepsilon$/dm$^3$ mol$^{-1}$ cm$^{-1}$ 69 000), 270 (31 000), 318 (15 000) and 343 (7700). Single crystals with the composition $[Ru(bpy)(CH_3CN)_2(dppcb)PdCl_2](SbF_6)_2\cdot 2H_2O$ suitable for an X-ray structure analysis were obtained by slow evaporation of a $CH_3CN$ solution of $[Ru(bpy)(CH_3CN)_2(dppcb)PdCl_2](SbF_6)_2$ (**8**) at ambient temperature. This crystallization was only successful under an atmosphere of air, since water molecules are incorporated into the crystal lattice. In this case the choice of $SbF_6^-$ anions was essential in order to obtain good quality single crystals. $[Ru(bpy)(CH_3CN)_2(dppcb)PdCl_2](SbF_6)_2$ has been prepared in an analogous manner starting from $[Ru(bpy)_2(dppcb)PdCl_2](SbF_6)_2$.

**$[Ru(bpy)(CH_3CN)_2(dppcb)Os(bpy)_2](PF_6)_4$ (9).** A 10 : 8 mixture[2b] of diastereoisomers (ΔΛ/ΛΔ)- and (ΔΔ/ΛΛ)-$[Ru(bpy)_2(dppcb)Os(bpy)_2](PF_6)_4$ (**5/6**; 0.0600 g, 0.0262 mmol) was dissolved in $CH_3CN$ (60 mL) and this solution was irradiated with an un-focused 700 W medium pressure Hg lamp with vigorous stirring for 68 h. The solvent was completely removed, the residue was suspended in $CH_2Cl_2$ (60 mL) and stirred for 16 h. An orange powder was filtered off, washed with $CH_2Cl_2$ and dried *in vacuo*. (Yield: 0.0331 g, 57.0%.) Mp > 300 °C. (Found: C 46.50, H 3.47, N 4.97, $C_{86}H_{74}F_{24}N_8P_8OsRu$ (2214.623) requires C 46.64, H 3.37, N 5.06%.) $^{31}P\{^1H\}$ NMR ($CH_3CN$): $\delta$ 80.4 (t, $^2J(P,P) + {}^3J(P,P)_{cis} = {}^3J(P,P)_{trans}$ = 11.0 Hz, $2P_{Ru}$), 46.8 (dd, $^2J(P,P) + {}^3J(P,P)_{cis}$ = 22.0 Hz, $^3J(P,P)_{trans}$ = 11.0 Hz, $P_{Os}$), 37.9 (dd, $^2J(P,P) + {}^3J(P,P)_{cis}$ = 22.0 Hz, $^3J(P,P)_{trans}$ = 11.0 Hz, $P_{Os}$), −143.2 (septet, $^1J(P,F)$ = 706 Hz, $PF_6^-$). $^1H$ NMR ($CD_3CN$): $\delta$ 9.72 (d, $^3J(H, H)$ = 6.0 Hz, 1 H, bpy-*H*), 9.02 (d, $^3J(H, H)$ = 5.0 Hz, 1 H, bpy-*H*), 8.54 (m, 1 H, bpy-*H*), 8.51 (m, 2 H, bpy-*H*), 8.37 (m, 2 H, bpy-*H*), 8.22 (m, 2 H, bpy-*H*), 8.02 (t, $^3J(H, H)$ = 5.0 Hz, 1H, bpy-*H*), 7.87 (m, 2 H, bpy-*H*), 7.78 (t, $^3J(H, H)$ = 5.0 Hz, 2 H, bpy-*H*), 7.63 (m, 2 H, bpy-*H*), 7.00–7.60 (m, 40 H, phenyl-*H*), 6.77 (m, 2 H, bpy-*H*), 6.64 (m, 2 H, bpy-*H*), 5.94 (m, 2 H, bpy-*H*), 5.87 (m, 2 H, bpy-*H*), 4.48 (br m, 2 H, C*H*), 4.07 (br m, 2 H, C*H*), 1.26 (s, 3 H, C*H*$_3$CN), 0.80 (s, 3 H, C*H*$_3$CN). Positive ion FAB-MS: *m*/*z* (*m*/*z*$_{calcd}$) 2069.9 (2069.7) $[M - PF_6]^+$, 1841.2 (1841.6) $[M - H - 2PF_6 - 2CH_3CN]^+$. UV-vis absorption: $\lambda_{max}$ ($1.2 \times 10^{-4}$ M in $CH_3CN$)/nm 230 ($\varepsilon$/dm$^3$ mol$^{-1}$ cm$^{-1}$ 28 000), 277 (19 000), 317 (11 000), 362 (4300) and 475 (1200). $E_{1/2}$ values *vs.* SCE ($\Delta E$, $\Delta E_p$ [mV]): $Ru^{II/III}$ +2.15 V [80], $Os^{II/III}$ +1.51 V [80], first $bpy^{0/-}$ −1.24 V [90], second $bpy^{0/-}$ −1.46 V [70], third $bpy^{0/-}$ −2.16 V [80]. Single crystals suitable for an X-ray structure analysis with the composition $[Ru(bpy)(CH_3CN)_2(dppcb)Os(bpy)_2](PF_6)_4\cdot 1.5$ $CH_3CN$ were obtained by gas-phase diffusion of $Et_2O$ into a $CH_3CN$ solution of **9** under an Ar atmosphere at ambient temperature.

## X-Ray crystallography†

Details of the crystals and data collections are summarized in Tables 1 and 2. The data collections were performed on a Nonius Kappa CCD diffractometer using combined $\phi$-$\omega$-scans. Cell refinement, data reduction, and the empirical absorption correction were done by Denzo and Scalepack programs.[16]

All structure determination calculations were carried out using SHELXTL-NT V6.1 including SHELXS-97[17] and SHELXL-97.[18] Final refinements on $F^2$ were carried out with anisotropic thermal parameters for all non-hydrogen atoms in all cases except for **9**. In the case of **9** all non-hydrogen atoms were anisotropically refined except for the non-coordinating $CH_3CN$ solvent molecules. The hydrogen atoms were included using a riding model with isotropic *U* values depending on the $U_{eq}$ of the adjacent non-hydrogen atoms except for some of the non-coordinating solvent molecules. Thus, the hydrogen atoms on C(6) of one of the $CH_2Cl_2$ solvent molecules and on O(1) of the water solvent molecule in structure **2** have been omitted due to substantial disorder in both solvent molecules. The same is true for C(7) of one of the $CH_2Cl_2$ solvent molecules in **3**, for O(1) and C(8) of the MeOH solvent molecule and for O(2) of the water solvent molecule in **4**, for O(1) and O(2) of the water solvent molecules in **8**, and for C(10) and C(18) of the $CH_3CN$ solvent molecules in **9**. Tables 3 and 4 contain selected bond distances and bond angles of all six crystal structures.

**Table 2** Crystallographic data for $[Ru(bpy)(CH_3CN)_2(dppcb)MCl_2](SbF_6)_2$ (M = Pt, **7**; Pd, **8**) and $[Ru(bpy)(CH_3CN)_2(dppcb)Os(bpy)_2](PF_6)_4$ (**9**)

| Compound | **7** | **8** | **9** |
|---|---|---|---|
| Chemical formula | $C_{66}H_{58}Cl_2F_{12}N_4P_6PtRu$ | $C_{66}H_{58}Cl_2F_{12}N_4P_6PdRu{\cdot}2H_2O$ | $C_{86}H_{74}F_{24}N_8P_8OsRu{\cdot}1.5CH_3CN$ |
| Formula weight | 1869.62 | 1812.94 | 2271.64 |
| Crystal system | Monoclinic | Monoclinic | Triclinic |
| Space group | $P2_1/c$ | $P2_1/c$ | $P\bar{1}$ |
| $a$/Å | 14.1694(3) | 14.4448(6) | 13.5536(4) |
| $b$/Å | 21.0307(4) | 21.0505(9) | 14.8181(4) |
| $c$/Å | 25.9245(3) | 26.0985(9) | 28.5615(7) |
| $\alpha$/° | — | — | 77.347(1) |
| $\beta$/° | 98.406(1) | 99.057(2) | 86.351(2) |
| $\gamma$/° | — | — | 63.021(1) |
| $U$/Å$^3$ | 7642.3(2) | 7836.8(5) | 4983.6(2) |
| $T$/K | 243 | 243 | 243 |
| $Z$ | 4 | 4 | 2 |
| Measured reflections | 32 735 | 24 437 | 28 777 |
| Independent reflections | 17 413 ($R_{int}$ = 0.0291) | 14 350 ($R_{int}$ = 0.0478) | 18 305 ($R_{int}$ = 0.0493) |
| Final $R_1$, w$R_2$ [$I > 2\sigma(I)$ **7**; $I > 3\sigma(I)$ **8**, **9**] | 0.0493, 0.1278 | 0.0625, 0.1632 | 0.0583, 0.1488 |

**Table 3** Selected bond lengths (Å) and angles (°) for $[Ru(bpy)_2(dppcb)MCl_2](PF_6)_2$ (M = Pt, **2**; Pd, **3**; Ni, **4**)

| Compound **2** | | | |
|---|---|---|---|
| Pt(1)–P(1) | 2.206(3) | Ru(1)–P(3) | 2.317(3) |
| Pt(1)–P(2) | 2.217(3) | Ru(1)–P(4) | 2.312(3) |
| Pt(1)–Cl(1) | 2.353(3) | Pt(1)–Cl(2) | 2.326(3) |
| C(1)–C(2) | 1.558(14) | Ru(1)–N(1) | 2.068(8) |
| C(1)–C(4) | 1.533(14) | Ru(1)–N(2) | 2.104(9) |
| C(2)–C(3) | 1.576(13) | Ru(1)–N(3) | 2.127(8) |
| C(3)–C(4) | 1.560(14) | Ru(1)–N(4) | 2.132(9) |
| P(1)–Pt(1)–P(2) | 88.70(11) | P(3)–Ru(1)–P(4) | 83.37(10) |
| N(1)–Ru(1)–N(2) | 78.7(3) | N(3)–Ru(1)–N(4) | 76.6(4) |
| **Compound 3** | | | |
| Pd(1)–P(1) | 2.2207(17) | Ru(1)–P(3) | 2.3195(16) |
| C(1)–P(2) | 2.2238(17) | Ru(1)–P(4) | 2.3199(19) |
| C(1)–Cl(1) | 2.346(2) | Pd(1)–Cl(2) | 2.3188(17) |
| C(2)–C(2) | 1.534(8) | Ru(1)–N(1) | 2.114(5) |
| C(1)–C(4) | 1.582(9) | Ru(1)–N(2) | 2.148(5) |
| C(2)–C(3) | 1.551(8) | Ru(1)–N(3) | 2.121(5) |
| C(3)–C(4) | 1.541(8) | Ru(1)–N(4) | 2.088(5) |
| P(1)–Pt(1)–P(2) | 87.82(6) | P(3)–Ru(1)–P(4) | 84.01(6) |
| N(1)–Ru(1)–N(2) | 77.2(2) | N(3)–Ru(1)–N(4) | 77.8(2) |
| **Compound 4** | | | |
| Ni(1)–P(1) | 2.1338(12) | Ru(1)–P(3) | 2.3231(11) |
| Ni(1)–P(2) | 2.1430(13) | Ru(1)–P(4) | 2.3277(12) |
| Ni(1)–Cll(1) | 2.1939(15) | Ni(1)–Cl(2) | 2.1696(13) |
| C(1))–C(2 | 1.560(6) | Ru(1)–N(1) | 2.111(3) |
| C(1))–C(4) | 1.553(5) | Ru(1)–N(2) | 2.127(4) |
| C(2))–C(3) | 1.551(5) | Ru(1)–N(3) | 2.120(3) |
| C(3)–C(4) | 1.548(6) | Ru(1)–N(4) | 2.096(3) |
| P(1)–Ni(1)–P(2) | 89.05(4) | P(3)–Ru(1)–P(4) | 84.18(4) |
| N(1)–Ru(1)–N(2) | 77.26(16) | N(3)–Ru(1)–N(4) | 77.54(13) |

**Table 4** Selected bond lengths (Å) and angles (°) for $[Ru(bpy)(CH_3CN)_2(dppcb)MCl_2](SbF_6)_2$ (M = Pt, **7**; Pd, **8**) and $[Ru(bpy)(CH_3CN)_2(dppcb)Os(bpy)_2](PF_6)_4$ (**9**)

| Compound **7** | | | |
|---|---|---|---|
| Pt(1)–P(3) | 2.212(2) | Ru(1)–P(1) | 2.325(2) |
| Pt(1)–P(4) | 2.215(2) | Ru(1)–P(2) | 2.321(2) |
| Pt(1)–Cl(1) | 2.335(2) | Pt(1)–Cl(2) | 2.351(2) |
| C(1)–C(2) | 1.575(9) | Ru(1)–N(1) | 2.060(7) |
| C(1)–C(4) | 1.554(10) | Ru(1)–N(2) | 1.996(7) |
| C(2)–C(3) | 1.554(10) | Ru(1)–N(3) | 2.133(6) |
| C(3)–C(4) | 1.560(9) | Ru(1)–N(4) | 2.142(6) |
| P(3)–Pt(1)–P(4) | 87.17(7) | P(1)–Ru(1)–P(2) | 81.48(7) |
| N(1)–Ru(1)–N(2) | 169.9(2) | N(3)–Ru(1)–N(4) | 76.5(3) |
| **Compound 8** | | | |
| Pd(1)–P(3) | 2.219(3) | Ru(1)–P(1) | 2.322(3) |
| C(1)–P(4) | 2.225(3) | Ru(1)–P(2) | 2.315(3) |
| Pd(1)–Cl(1) | 2.338(4) | Ru(1)–Cl(2) | 2.356(3) |
| C(1)–C(2) | 1.550(15) | Ru(1)–N(1) | 2.081(10) |
| C(1)–C(4) | 1.565(17) | Ru(1)–N(2) | 2.006(12) |
| C(2)–C(3) | 1.546(15) | Ru(1)–N(3) | 2.131(10) |
| C(3)–C(4) | 1.545(15) | Ru(1)–N(4) | 2.122(10) |
| P(3)–Pd(1)–P(4) | 86.13(12) | P(1)–Ru(1)–P(2) | 81.25(11) |
| N(1)–Ru(1)–N(2) | 170.5(4) | N(3)–Ru(1)–N(4) | 76.1 |
| **Compound 9** | | | |
| Os(1)–P(1) | 2.321(3) | Ru(1)–P(3) | 2.326(3) |
| Os(1)–P(2) | 2.318(3) | Ru(1)–P(4) | 2.306(3) |
| Os(1)–N(1) | 2.096(8) | Ru(1)–N(5) | 2.048(11) |
| Os(1)–N(2) | 2.119(8) | Ru(1)–N(6) | 2.003(13) |
| Os(1)–N(3) | 2.118(8) | Ru(1)–N(7) | 2.128(11) |
| Os(1)–N(4) | 2.083(7) | Ru(1)–N(8) | 2.149(11) |
| C(1)–C(2) | 1.564(13) | C(2)–C(3) | 1.553(14) |
| C(1)–C(4) | 1.557(13) | C(3)–C(4) | 1.571(13) |
| P(1)–Os(1)–P(2) | 85.79(9) | P(3)–Ru(1)–P(4) | 82.55(10) |
| N(1)–Os(1)–N(2) | 77.2(3) | N(5)–Ru(1)–N(6) | 172.2(4) |
| N(3)–Os(1)–N(4) | 77.7(3) | N(7)–Ru(1)–N(8) | 75.9(5) |

## Results and discussion

### Synthesis of the complexes and investigation in solution

The general route for the synthesis of heterodinuclear compounds is given by the separate preparation of a bridging ligand, and of the mononuclear metal complex precursors.[19] In contrast to the drawbacks of the synthesis of other rigid, rod-like bridging ligands as a consequence of their insolubility in organic solvents,[19] dppcb is very well soluble in THF and can easily be purified.[6] A suitable entropy effect due to the threefold excess of dppcb, together with a high dilution technique combined with the slow addition of *cis*-$[RuCl_2(bpy)_2]{\cdot}2H_2O$ leads to a synthetic protocol that allows the production of $[Ru(bpy)_2(dppcb)]X_2$ (**1**; X = $PF_6$, $SbF_6$) in excellent yield (see Scheme 1).[4b,19] Even the excess of

 

dppcb can be removed after the synthesis of **1** and used again. The X-ray structure of **1** clearly reveals its diastereotopicity[5a] and hence also in solution **1** shows four distinct $^{31}P\{^1H\}$ NMR signals. The singlets at 76.0 and 73.0 are attributed to the phosphorus atoms of dppcb attached to $Ru^{II}$, whereas the resonances of the "free" phosphines in **1** occur at –7.9 and –10.1, respectively.[5a] The latter signals are doublets and show a typical large $^3J(P,P)_{cis}$ coupling of 117.0 Hz, that is comparable to the corresponding parameter of 98.9 Hz for the completely "free" ligand dppcb.[6] It is well-known that $^3J(P,P)$ values are conformationally dependent and the variations in $^3J(P,P)$ arise mainly from lone-pair orientation effects determined by steric interactions.[7a,20] Obviously, these large couplings disappear as a consequence of coordination, since for the $RuP_2$ moiety in **1** singlets are observed.

The reaction of **1** with $[PtCl_2(\eta^4\text{-COD})]$ produces $[Ru(bpy)_2(dppcb)PtCl_2]X_2$ (**2**; X = $PF_6$, $SbF_6$) as yellow micro-crystalline powder in 75.0% yield (Scheme 1). The analogous reaction of **1** with $[PdCl_2(\eta^4\text{-COD})]$ proceeds similarly leading to $[Ru(bpy)_2(dppcb)PdCl_2]X_2$ (**3**; X = $PF_6$, $SbF_6$) as yellow micro-crystalline powder in 64.1% yield. In the case of $[Ru(bpy)_2(dppcb)NiCl_2]X_2$ (**4**; X = $PF_6$, $SbF_6$), **1** was reacted with $[NiCl_2(DME)]$ producing **4** as red crystals in 58.0% yield. The new heterodimetallic complexes **2–4** were authenticated by multinuclear NMR spectroscopy, ESI-MS measurements, UV-vis and luminescence spectroscopy, excited state lifetimes and cyclic voltammetry in solution. Furthermore, in the solid state all three single-crystal X-ray structures of **2–4** (*vide infra*) and the corresponding elemental analyses are given. As in the case of **1**, these X-ray structures show the diastereotopicity of **2–4** and therefore four different $^{31}P\{^1H\}$ NMR resonances occur in solution for each complex. **2** exhibits the signals attributed to the phosphorus atoms of dppcb attached to $Ru^{II}$ at 85.7 and 83.7, respectively (see Scheme 1). The former resonance is a doublet of doublets due to $^2J(P,P) + {}^3J(P,P)_{cis}$ of 10.4 Hz and $^3J(P,P)_{trans}$ of 12.0 Hz. The latter signal shows a doublet of triplets in accordance with the equivalence of $^2J(P,P) + {}^3J(P,P)_{cis}$ and $^3J(P,P)_{trans}$ being 10.4 Hz and the occurrence of a further splitting due to $^4J(P,P)_{trans}$ of 5.9 Hz. The resonances at 54.5 and 52.7 can be clearly assigned to the phosphorus atoms of dppcb attached to $Pt^{II}$, since they exhibit $^1J(Pt,P)$ couplings of 3652 and 3659 Hz, respectively. The former signal shows a doublet of doublets and the latter a doublet of triplets for the same reasons as for the $RuP_2$ moiety, where $^2J(P,P) + {}^3J(P,P)_{cis}$ is 12.0 Hz for the $PtP_2$ moiety. In the $^{195}Pt\{^1H\}$ NMR spectrum the doublet of doublets at –4520 is also completely in line with the diastereotopicity of **2**. By analogy with **2**, the resonances at 86.3 and 85.6 in the $^{31}P\{^1H\}$ NMR spectrum of **3** can be easily attributed to the phosphorus atoms of dppcb attached to $Ru^{II}$ (see Scheme 1). As in the case of **2** the former signal is a doublet of doublets due to $^2J(P,P) + {}^3J(P,P)_{cis}$ of 11.0 Hz and $^3J(P,P)_{trans}$ of 13.0 Hz and the latter signal is a doublet of triplets, where $^3J(P,P)_{trans}$ of 11.0 Hz is identical with $^2J(P,P) + {}^3J(P,P)_{cis}$ and this resonance is further split *via* $^4J(P,P)_{trans}$ of 7.0 Hz. The remaining two signals at 76.1 and 75.3 are assigned to the phosphorus atoms of dppcb attached to $Pd^{II}$, where a downfield shift of about 20 ppm of these resonances compared with their $Pt^{II}$ analogues (*vide supra*) is typical.[6,21] Since $^2J(P,P) + {}^3J(P,P)_{cis}$ is 11.0 Hz for the $PdP_2$ moiety, the corresponding signals occur as doublet of doublets of doublets and as triplet, respectively. By analogy with **2** and **3**, the resonances at 86.3 and 84.8 in the $^{31}P\{^1H\}$ NMR spectrum of **4** are attributed to the $RuP_2$ moiety (see Scheme 1). Both signals are triplets, since in both cases $^2J(P,P) + {}^3J(P,P)_{cis}$ is identical with $^3J(P,P)_{trans}$ of 11.0 Hz. For the $NiP_2$ moiety, the resonances at 68.7 and 66.2, respectively, are doublets of doublets due to $^2J(P,P) + {}^3J(P,P)_{cis}$ of 64.0 Hz, where their shifts are typical of five-membered metallacycles formed of dppcb and $NiCl_2$.[22] It is important to emphasize at this point, that the $^{31}P\{^1H\}$ NMR parameters of the novel heterodimetallic complexes **2–4** reflecting their solution structures are consistent and completely in line with their solid state X-ray structures (*vide infra*).

The reaction of **1** with *cis*-$[OsCl_2(bpy)_2]$ leads to a 10 : 8 mixture of diastereoisomers (ΔΛ/ΛΔ)- and (ΔΔ/ΛΛ)-$[Ru(bpy)_2(dppcb)Os(bpy)_2](PF_6)_4$ (**5/6**) as light orange powder in 56.0% yield (Scheme 1; 10 : 8 = **5**:**6**; this ratio was determined by $^{31}P\{^1H\}$ and $^1H$ NMR spectroscopy leading to the same result).[2b] Compounds **5** and **6** were separated by partial crystallization *via* gas-phase diffusion of $CH_2Cl_2$ into a $CH_3CN$ solution of **5/6** under an Ar atmosphere at ambient temperature. The formation of pure single crystals containing only **5** is the thermodynamic driving force.[5b] The crystal structure of **5** clearly reveals the presence of two different chiral centres[2b] and therefore also in solution **5** shows four distinct $^{31}P\{^1H\}$ NMR signals. By analogy with **1–4**, the resonances at 80.1 and 75.2 are assigned to the phosphorus atoms of dppcb attached to $Ru^{II}$ (see Scheme 1). They occur as doublets of triplets due to the equality of $^2J(P,P) + {}^3J(P,P)_{cis}$ and $^3J(P,P)_{trans}$ of 8.9 Hz and a further splitting by $^4J(P,P)_{trans}$ of 3.0 Hz. In agreement with the $^{31}P\{^1H\}$ NMR shifts for the homodimetallic species *meso*-(ΔΛ/ΛΔ)- or *rac*-(ΔΔ/ΛΛ)-$[Os_2(dppcb)(bpy)_4](PF_6)_4$,[2b] the signals at 38.8 and 35.4 are attributed to the $OsP_2$ moiety of **5**. They are also doublets of triplets as a consequence of the same coupling parameters as observed for the $RuP_2$ moiety. The second diastereoisomer **6** shows an analogous coupling pattern, where the resonances assigned to the $RuP_2$ moiety occur at 77.3 and 76.4 and the signals for the $OsP_2$ moiety at 35.6 and 34.9, respectively. All four resonances are doublets of triplets as in the case of **5** due to the equality of $^2J(P,P) + {}^3J(P,P)_{cis}$ and $^3J(P,P)_{trans}$ of 8.9 Hz and a further splitting by $^4J(P,P)_{trans}$ of 5.9 Hz.

Though the "steric pressure"[2b,5,7] is quite different for the complexes **2**, **3**, and **5** (*vide infra*), they exhibit a surprisingly consistent photochemical reactivity. Thus, irradiating **2**, **3** or **5/6** dissolved in $CH_3CN$ with visible light leads to the analogous compounds $[Ru(bpy)(CH_3CN)_2(dppcb)MCl_2]X_2$ (M = Pt, **7**; Pd, **8**; X = $PF_6$, $SbF_6$) and $[Ru(bpy)(CH_3CN)_2(dppcb)Os(bpy)_2](PF_6)_4$ (**9**; see Scheme 2) in 55.0%, 36.0%, and 57.0% yields, respectively. However, the "steric pressure" in **4** is obviously too low and no clean photoreaction is observed, where also electronic factors cannot be ruled out. This different photochemical behaviour is completely in line with the photophysical properties of **2–4** and **5/6** (*vide infra*). The crystal structures of **7** and **8**, also given in this work for the first time, clearly indicate that diastereotopicity is lost and hence only two distinct $^{31}P\{^1H\}$ NMR signals occur for each complex. In the case of **7** the resonances at 79.3 and 58.3 belong to the $RuP_2$ and $PtP_2$ moieties, respectively, where the latter signal shows a $^1J(Pt,P)$ coupling of 3618 Hz (see Scheme 2). Both resonances are triplets due to the equivalence of both $^2J(P,P) + {}^3J(P,P)_{cis}$ couplings and $^3J(P,P)_{trans}$ of 12.0 Hz. For **8** the signal at 80.7 is attributed to the phosphorus atoms of dppcb attached to $Ru^{II}$ and the resonance at 79.0 to the $PdP_2$ moiety. The latter signal

is slightly broadened, this effect being typical of $PdP_2$ but not of $RuP_2$ moieties within this series of compounds **1–9**. The coupling pattern of **8** is identical with **7**. However, the crystal structure of **9** (*vide infra*) clearly reveals that diastereotopicity is retained and therefore two resonances occur within the characteristic region of $OsP_2$ at 46.8 and 37.9 (see Scheme 2). Nevertheless, the signals assigned to the $RuP_2$ moiety at 80.4 coincide and a single triplet is observed as a consequence of the equality of $^2J(P,P) + {}^3J(P,P)_{cis}$ and $^3J(P,P)_{trans}$ of 11.0 Hz. The $OsP_2$ resonances are doublets of doublets in line with $^2J(P,P) + {}^3J(P,P)_{cis}$ of 22.0 Hz. Also in the case of the new heterodimetallic complexes **7–9** the $^{31}P\{^1H\}$ NMR parameters reflecting their solution structures are consistent and completely in agreement with their single-crystal X-ray structures. It is important to note at this point, that the species **7–9** containing the $[Ru(bpy)(CH_3CN)_2]^{2+}$ chromophore with a *trans* arrangement of the $CH_3CN$ ligands are unique, since this chromophore can only be achieved *via* a photochemical ligand exchange reaction.[2b,5]

### Crystal structures of $[Ru(bpy)_2(dppcb)MCl_2](PF_6)_2$ (M = Pt, 2; Pd, 3; Ni, 4)

To the best of our knowledge the crystal structures of **2–4** are the first structures of heterodimetallic complexes, where octahedral $[Ru(bpy)_2]^{2+}$ chromophores and square-planar metal centres are combined with a tetraphosphine. The asymmetric unit of the crystal structure of **2**·3.5$CH_2Cl_2$·0.5$H_2O$ contains the metal complex cation, two $[PF_6]^-$ anions, 3.5 molecules of dichloromethane, and half a molecule of water. One dichloromethane molecule and the water molecule were disordered. Similar to this, the asymmetric unit of the crystal structure of **3**·1.3$CH_2Cl_2$·$H_2O$ consists of the metal complex cation, two $[PF_6]^-$ anions, 1.3 molecules of dichloromethane, and one molecule of water. Two of the three independent dichloromethane molecules and the water molecule were disordered. This means that the solid-state structures of **2** and **3** are not isomorphous in the strict sense of the word.[7a,8,23] Nevertheless, they are essentially the same with respect to the conformations of the coordinated ligands, the packing of the cations and the relative positions of the $[PF_6]^-$ anions in the lattice.

A view of **3** is shown in Fig. 1 and Table 3 contains selected bond lengths and angles of **2** and **3**. It is important to study the "steric pressure" in **2–4**,[2b,5] since non-radiative decay for these molecules is typically dominated by energy loss into a series of medium-frequency ring-stretching vibrations with energy spacings between 1000 and 1600 $cm^{-1}$ (*vide infra*).[24] Thus, the shortest intramolecular contacts between a bpy ligand and a phenyl ring are 2.346 Å in **2** and 2.282 Å in **3**. The analogous contacts between the phenyl rings along a *trans* axis of the cyclobutane rings are 2.951 Å in **2** and 2.905 Å in **3**. These contact approaches are indicative of high "steric pressure".[2b,5,7,25] Typically, this "steric pressure" is partially released *via* "envelope" folding of the five-membered metallacycles in **2** and **3** (see Fig. 1). The corresponding folding angles are 164.8(3)° and 159.5(3)° in **2** and are the dihedral angles between the least-squares planes through the atoms P(1), C(1), C(2), P(2) and P(1), Pt(1), P(2), and through P(3), C(3), C(4), P(4) and P(3), Ru(1), P(4), respectively. The analogous folding angles are 165.81(17)° and 159.46(19)° in **3** and are identical with **2** within statistical significance due to the nearly isomorphous

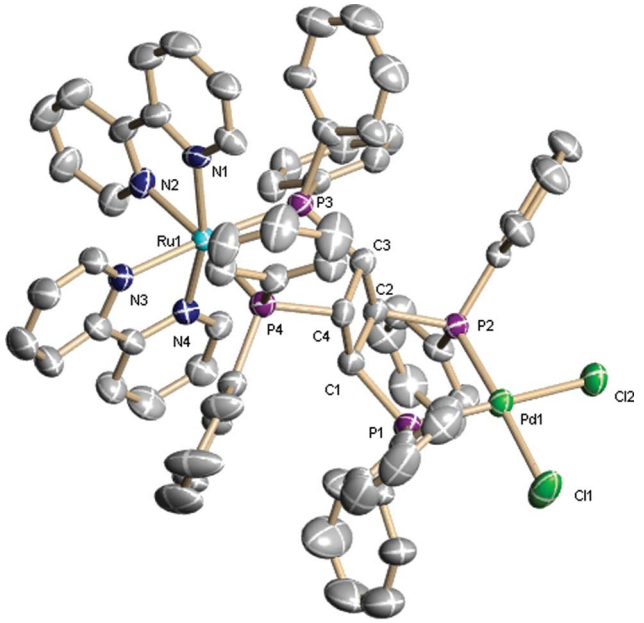


**Fig. 1** ORTEP diagram of the cation of **3**·1.3$CH_2Cl_2$·$H_2O$ with 30% probability ellipsoids. The $CH_2Cl_2$ molecules, the water molecule, and the hydrogen atoms are omitted for clarity.

crystal structures. All foldings occur towards the cyclobutane rings (Fig. 1).

However, these similar crystal structures also allow comparison of the radii of Pt and Pd atoms.[8] Typically, the mean value of the Pt–P bond lengths of 2.211(2) Å in **2** is significantly shorter than the mean value of the Pd–P bond lengths of 2.2223(12) Å in **3** (see Table 3).[8] The deviations of the platinum and palladium atoms in **2** or **3** from the coordination planes, defined by P(1), P(2), Cl(1) and Cl(2), are 0.053(1) Å for Pt(1) and 0.092(1) Å for Pd(1). They occur towards the cyclobutane rings and are also significantly different. Furthermore, the cyclobutane ring in **2** is planar within statistical significance, whereas in **3** the deviations from a least-squares plane through the cyclobutane ring are 0.025(3) Å for C(1) and C(3), and –0.025(3) Å for C(2) and C(4). Obviously, the actual conformations of **2** and **3** are the result of a subtle balance between intramolecular contact approaches, "envelope" or cyclobutane ring folding and differences in square-planar stabilization energies. At this point it is important to note, that these subtle differences control the lifetimes of the related excited states of **2** and **3** and their efficiency of Ru(II) luminescence (*vide infra*).[2b,5,26]

The asymmetric unit of the crystal structure of **4**·2.7$CH_2Cl_2$·$H_2O$·MeOH contains the metal complex cation, two $[PF_6]^-$ anions, 2.7 molecules of dichloromethane, one molecule of water, and one molecule of MeOH. One dichloromethane molecule, the water molecule, and the MeOH molecule were disordered. A view of **4** is shown in Fig. 2 and Table 3 contains selected bond lengths and angles. Interestingly, though the packing of the cations and the relative positions of the $[PF_6]^-$ anions in the lattice of **4** are completely different from **2** and **3**, only slight variations in the conformations of the coordinated ligands can be observed, when **2** or **3** are compared with **4** (see Fig. 1 and 2). It seems likely, that the room to move with respect to the overall conformations of **2–4** is restricted as a consequence

 

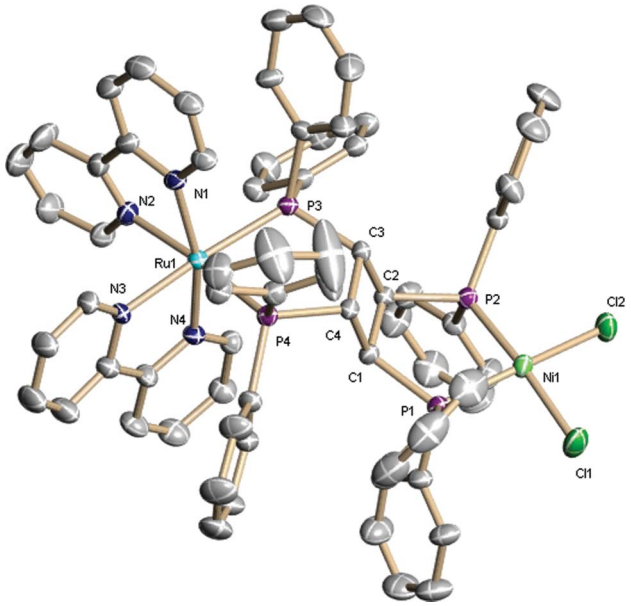


**Fig. 2** ORTEP diagram of the cation of **4**·2.7$CH_2Cl_2$·$H_2O$·MeOH with 30% probability ellipsoids. The $CH_2Cl_2$ molecules, the water molecule, the MeOH molecule and the hydrogen atoms are omitted for clarity.

of the high "steric pressure" in these molecules. This is confirmed by the shortest intramolecular contact between a bpy ligand and a phenyl ring of 2.251 Å in **4**. The analogous contact between the phenyl rings along a *trans* axis of the cyclobutane ring is 2.909 Å. However, as before subtle differences to **2** or **3** are present in the very conformation of **4**. Thus, the "envelope" folding angle of the square-planar coordination unit in **4** of 166.64(13)° is significantly larger than the corresponding parameter in **2** and defined by the dihedral angle between the least-squares planes through the atoms P(1), C(1), C(2), P(2) and P(1), Ni(1), P(2), respectively (Fig. 2). By contrast, the analogous "envelope" foldings of **3** and **4** are identical within statistical significance. The same is true for the "envelope" foldings of the octahedral coordination units in **2**–**4**, showing identical values within statistical significance, where the corresponding parameter for **4**, defined as above, is 159.30(13)°. Also in **4** both "envelope" foldings occur towards the cyclobutane ring. The deviation of the nickel atom in **4** from the coordination plane, defined as above, is 0.095(1) Å towards the cyclobutane ring and hence significantly larger than the analogous value of **2**, but identical with **3** within statistical significance. However, only in **4** a significant tetrahedral distortion is present, showing symmetrical tetrahedral deviations of 0.009(1) Å from the coordination plane. As in the case of **3**, but in contrast to **2**, the cyclobutane ring is not completely planar in **4**, where the deviations from a least-squares plane through the cyclobutane ring are 0.016(2) Å for C(1) and C(3), and –0.016(2) Å for C(2) and C(4). Obviously, the square-planar coordination unit in **4** showing a tetrahedral distortion is more flexible than in **2** and **3**, being in line with a reduction of the square-planar stabilization energy in Ni(II) compared with Pt(II) and Pd(II). This has dramatic consequences for the photochemical and photophysical properties of **2**–**4** (*vide infra*).

### Crystal structures of $[Ru(bpy)(CH_3CN)_2(dppcb)MCl_2](SbF_6)_2$ (M = Pt, 7; Pd, 8) and $[Ru(bpy)(CH_3CN)_2(dppcb)Os(bpy)_2](PF_6)_4$ (9)

The compounds **7**–**9** contain the unique chromophore *trans*-$[Ru(bpy)(CH_3CN)_2]^{2+}$ (see Scheme 2). When combined with dppcb, this chromophore has been prepared by our working group for the first time, following a photochemical synthetic protocol.[2b,5] **7**–**9** are the first heterodimetallic complexes containing this chromophore. Therefore, in order to understand their photophysical behaviour, it is necessary to study their X-ray structures.

The asymmetric unit of the crystal structure of **7** contains the metal complex cation and two $[SbF_6]^-$ anions, where one of the anions was disordered. By contrast, the asymmetric unit of the crystal structure of **8**·2$H_2O$ consists of the metal complex cation, two $[SbF_6]^-$ anions, and two disordered molecules of water. Nevertheless, the overall conformations of the cations of **7** and **8** are essentially the same (see Fig. 3). Table 4 contains selected bond lengths and angles of **7** and **8**. Obviously, as in the cases of **2**–**4** the room to move is restricted in **7** and **8** as a consequence of the high "steric pressure" also in these molecules. Indeed, the shortest intramolecular contacts between a bpy ligand and a phenyl ring are 2.563 Å in **7** and 2.528 Å in **8**. The analogous contacts between the phenyl rings along a *trans* axis of the cyclobutane rings are 3.093 Å in **7** and 2.759 Å in **8**. This high "steric pressure" is again partially released by "envelope" folding of the five-membered metallacycles towards the cyclobutane rings in **7** and **8** (see Fig. 3). Interestingly, the "envelope" folding angles of the square-planar coordination units, defined as above, are 156.6(2)° in **7** and 156.7(3)° in **8** and therefore identical within statistical significance. The same is true for the corresponding parameters of 147.42(16)° in **7** and 146.87(26)° in **8** of the octahedral coordination units. However, the deviation of the platinum atom in **7** from the coordination plane, defined as above, is 0.066(1) Å towards the cyclobutane ring and significantly smaller than the analogous value of 0.085(1) Å in **8**. In contrast to **7**, **8** shows a significant tetrahedral distortion with a mean tetrahedral deviation of 0.026(1) Å from the coordination plane. As in the case of **2**, the cyclobutane ring in **7** is planar within statistical significance. However, in **8** the deviations from a least-squares plane through the cyclobutane ring are 0.026(6) Å for C(1) and C(3), and –0.026(6) Å for C(2) and C(4). The subtle differences between the structural parameters of **7** and **8** are in agreement with a reduction of the square-planar stabilization energy in Pd(II) compared with Pt(II). Furthermore, a comparison of the X-ray structures of **2** and **3** with **7** and **8** (see Fig. 1 and Fig. 3) clearly reveals that the stretching vibration modes of $CH_3CN$, present only in **7** and **8**, cannot be directly influenced by "steric pressure". This leads to an enhancement of the non-radiative decay of the excited states of **7** and **8** and hence to a dramatic reduction of the luminescence lifetimes at ambient temperature of **7** and **8** compared with **2** and **3** (*vide infra*).

In the case of the diastereoisomers (ΔΛ/ΛΔ)- and (ΔΔ/ΛΛ)-$[Ru(bpy)_2(dppcb)Os(bpy)_2](PF_6)_4$ (**5**/**6**; see Scheme 1) the $^3$MLCT states are in thermal equilibrium with a Ru-centred upper lying d → d excited level, where the Os-centre cannot enter into play.[2b,27] This means that the osmium centre should remain photochemically inactive. The crystal structure of the photoproduct **9** (see Scheme 2), obtained by irradiating **5**/**6** in $CH_3CN$, is the unique

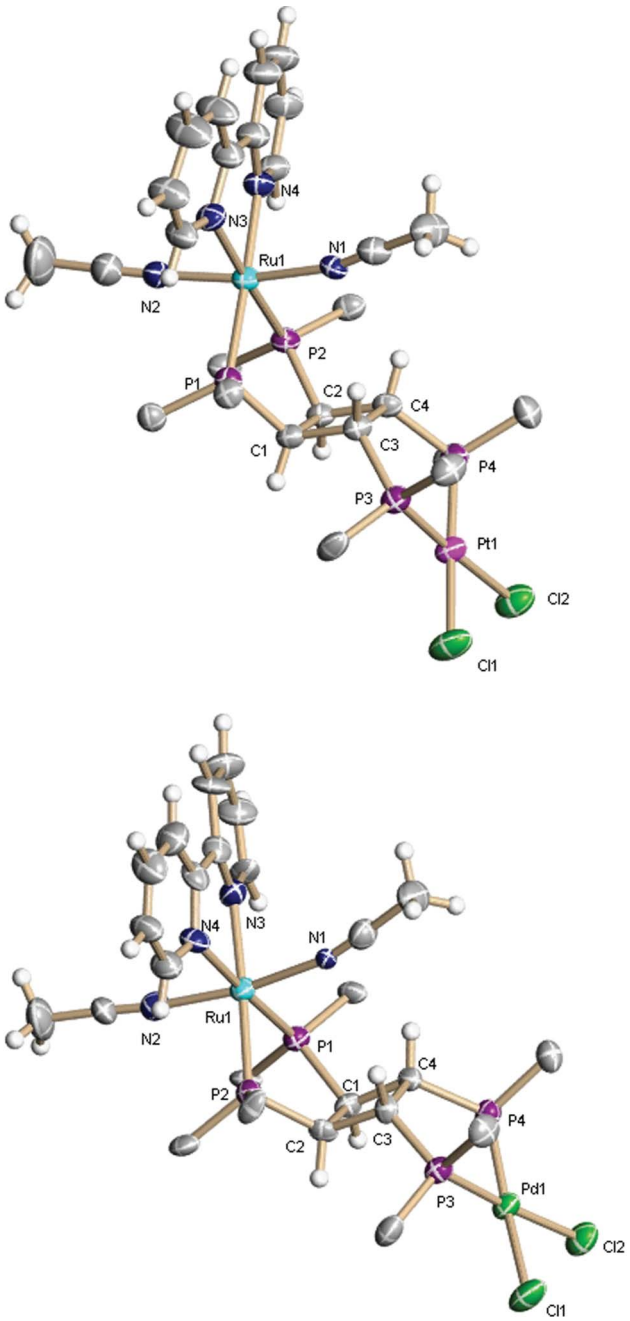


**Fig. 3** ORTEP diagrams of the cations of **7** (above) and **8**·2$H_2O$ (below) with 30% probability ellipsoids. The water molecules are omitted for clarity and only the *ipso* carbon atoms of the phenyl units are shown.

proof that the energy gap between $^3$MLCT and d → d excited states is much larger in the $Os^{II}$ complexes than in the $Ru^{II}$ complexes.

Views of **9** are shown in Fig. 4 and Table 4 contains selected bond lengths and angles. The asymmetric unit of the crystal structure of **9** consists of the metal complex cation, four $[PF_6]^-$ anions, and two disordered $CH_3CN$ solvent molecules. Since **9** contains a Ru-centre, also in this case "steric pressure" could control its photophysical properties given below.[2b,5] For this Ru-centre the shortest intramolecular contact between a bpy ligand and a phenyl ring is 2.263 Å. The corresponding contact for the Os-centre is 2.222 Å. The shortest intramolecular contact between the phenyl rings along a *trans* axis of the cyclobutane ring is 2.775 Å. However, the most astonishing feature of the crystal structure of **9** is, how the obvious high "steric pressure" is partially released by "envelope" folding of the five-membered metallacycles. Fig. 4 (right) shows that this folding occurs towards the cyclobutane ring for the Ru-centre, but away from the cyclobutane ring for the Os-centre, where this latter folding is typical of high "steric pressure".[5b] The corresponding "envelope" folding angles, defined as above, are 152.05(16)° for the Ru-centre and 160.45(31)° for the Os-centre. The deviations from a least-squares plane through the cyclobutane ring are 0.023(5) Å for C(1) and C(3), and –0.023(5) Å for C(2) and C(4). The common feature of compounds **7–9** is that they all contain the chromophore *trans*-$[Ru(bpy)(CH_3CN)_2]^{2+}$, where its excited state energy can be released by stretching vibrations of $CH_3CN$, that cannot be blocked by "steric pressure". However, only **9** contains a second chromophore, namely $[Os(bpy)_2]^{2+}$, showing a large energy gap between $^3$MLCT and d → d excited states.[2b,27] This means that as in the cases of **2** and **3**, but in contrast to **7** and **8**, **9** should again exhibit a long excited state lifetime at ambient temperature (*vide infra*).

### Absorption and emission spectra

The absorption spectra are shown in Fig. S14 and S15 (ESI, page S12).† For the new complexes **2–4** there are intense π, π* absorption bands in the UV region of the absorption spectra. They are due to intraligand (IL) transitions localized on the 2,2′-bipyridyl ligands of the $[Ru(bpy)_2]^{2+}$ chromophore.[28] The maxima occur at 271 (**2**; $\varepsilon$ = 34 000 $dm^3$ $mol^{-1}$ $cm^{-1}$), 269 (**3**; $\varepsilon$ = 37 000), and 277 nm (**4**; $\varepsilon$ = 24 000). In the case of **2** the transitions centred at 303 ($\varepsilon$ = 22 000) and 323 nm ($\varepsilon$ = 13 000) are attributed to the metal-centred (MC) d → d transitions of the Ru centre.[12a,14,29] For **3**, the analogous absorption bands occur at 293 ($\varepsilon$ = 21 000) and 324 nm ($\varepsilon$ = 15 000) and for **4** at 324 nm ($\varepsilon$ = 8900). Typically, the low-energy MLCT (Ru → bpy) transitions are observed at 377 (**2**; $\varepsilon$ = 6800), 356 (**3**; $\varepsilon$ = 7400), and 378 nm (**4**; $\varepsilon$ = 5700). This MLCT state is predominantly singlet in character.[4b] However, the coupling of M(II) (M = Pt, Pd, Ni) in **2–4** to Ru(II) in bis(bidentate) coordination environments to produce heterodimetallic complexes leads to systems that possess further stabilized MLCT excited states (predominantly triplet in character) relative to the homodimetallic analogs, $[Ru_2(dppcb)(bpy)_4]^{4+}$.[30] This orbital splitting is responsible for a low-energy tailing of the MLCT absorption bands extending to *ca.* 500 nm for **2** and **3**. In the case of **4** a pronounced further MLCT transition (predominantly triplet in character) occurs at 475 nm ($\varepsilon$ = 1200) extending to *ca.* 550 nm.

Also the novel compounds **7** and **8** show intense π, π* absorption bands in the UV region of the absorption spectra. They are attributed to intraligand (IL) transitions localized on the 2,2′-bipyridyl and $CH_3CN$ ligands of the *trans*-$[Ru(bpy)(CH_3CN)_2]^{2+}$ chromophore.[28] For **7** the maxima occur at 233 ($\varepsilon$ = 49 000) and 270 nm ($\varepsilon$ = 17 000) and for **8** at 233 ($\varepsilon$ = 69 000) and 270 nm ($\varepsilon$ = 31 000). Both transitions centred at 318 (**7**; $\varepsilon$ = 9100; **8**; $\varepsilon$ = 15 000) again stem from the metal-centred (MC) d → d transitions.[12a,14,29] However, the MLCT (Ru → bpy) transitions of **7** and **8** are blue shifted compared with **2–4**. They are observed as a shoulder centered at about 347 (**7**; $\varepsilon$ = 3300) and as a maximum at 343 nm (**8**; $\varepsilon$ = 7700). This MLCT state is again predominantly singlet in

 

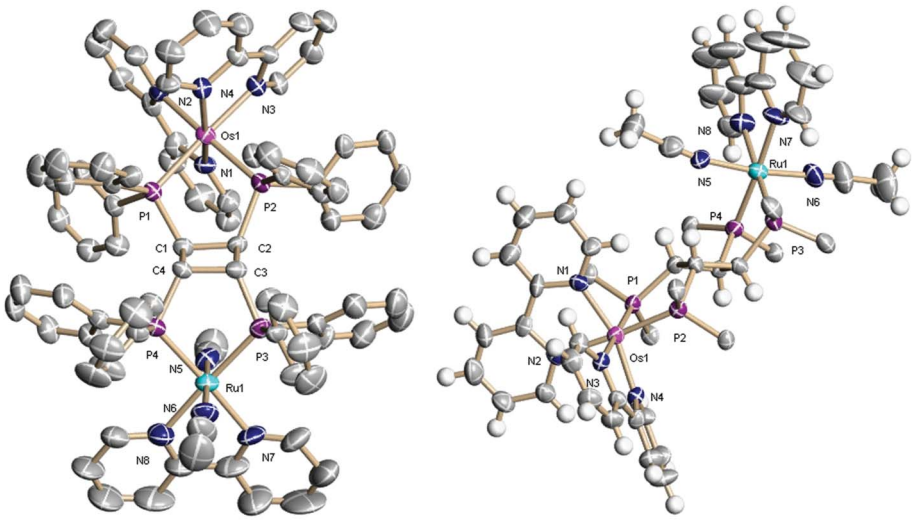


**Fig. 4** ORTEP diagrams of the cation of **9**·1.5$CH_3CN$ with 30% probability ellipsoids. The non-coordinated $CH_3CN$ molecules are omitted for clarity. Left: the hydrogen atoms are omitted. Right: only the *ipso* carbon atoms of the phenyl units are shown.

character.[4b] However, for the same reasons as in the cases **2–4** (*vide supra*) low-energy tailing of the MLCT absorption bands in **7** and **8** extends to *ca.* 450 nm.[30]

The unique species **9** shows intraligand (IL) transitions localized on the 2,2′-bipyridyl and $CH_3CN$ ligands of the *trans*-$[Ru(bpy)(CH_3CN)_2]^{2+}$ and $[Os(bpy)_2]^{2+}$ chromophores.[28] They occur at 230 ($\varepsilon$ = 28 000) and 277 nm ($\varepsilon$ = 19 000). As before, the transition centred at 317 nm ($\varepsilon$ = 11 000) is attributed to the metal-centred (MC) d → d transition.[12a,14,29] However, two MLCT (Ru → bpy and Os → bpy) absorption bands are observed for **9**. The transition at 362 nm ($\varepsilon$ = 4300) is typical of the *trans*-$[Ru(bpy)(CH_3CN)_2]^{2+}$ chromophore and comparable to the corresponding transitions in **7** and **8**. The low-energy MLCT (Os → bpy) absorption occurs at 475 nm ($\varepsilon$ = 1200) and is predominantly singlet in character.[2b,4,27] For the same reasons as above low-energy tailing of this MLCT absorption band extends to *ca.* 600 nm.[30]

The emission spectra of **2–4** and **7–9** are shown as ESI† (pages S4–S9), where an example is given below for the case of **9** (see Fig. 5). The emission centred at 560 nm for $\lambda_{ex}$ of 500 nm of **2** in a 4 : 1 : 2 (v/v) EtOH–MeOH–$CH_3CN$ glass at 77 K stems from the $^3$MLCT state (see Fig. S2, page S4†).[2b,5,31] This is confirmed by the analogous emissions under identical conditions at 529 nm for $\lambda_{ex}$ of 465 nm of **3** and at 521 nm for $\lambda_{ex}$ of 430 nm of **4** belonging to the same $[Ru(bpy)_2]^{2+}$ chromophore (see Fig. S4–S5, pages S5, S6†). Furthermore, the appearance of vibrational progression is typical for this kind of chromophore.[2b,5a,12a,13] However, at 298 K only for **3** the expected red shift of the emission from the $^3$MLCT state is observed, occurring at 600 nm for $\lambda_{ex}$ of 465 nm in $CH_3CN$ (see Fig. S3, page S5†).[2b,5a]

Instead of that for **2** the emission centred at 550 nm for $\lambda_{ex}$ of 530 nm in $CH_3CN$ at 298 K is blue shifted compared with the transition at 77 K (see Fig. S1 and S2, page S4†). Especially the lifetime measurements of compound **2** clearly indicate that two emissions are present (see Table 1 of the ESI†). The unusual temperature shift of the emissions (compare Fig. S1 and S2 of the ESI†) should also be regarded as proof positive that two emissions are involved: typically the long component $^3$MLCT emission is very strong at 77 K and therefore dominates the emission band at 77 K. This emission becomes considerably weaker at ambient temperature and at this temperature the short component of the emission dominates the emission band. Due to its very short lifetime at 77 K this emission is clearly no $^3$MLCT emission. Therefore it is not the same transition at 77 and 298 K, respectively, that dominates the emission band. This is comparable to the case of $[Ru(dppcbO_2)(bpy)_2](PF_6)_2$,[5a] where $dppcbO_2$ is *cis*,*trans*,*cis*-1,2-bis(diphenylphosphinoyl)-3,4-bis(diphenylphosphino)cyclobutane and a second short component of the emission of this complex is due to the introduction of phosphinoyl groups. For **2** this second short component stems from the $Pt^{II}$ centre, since it is neither present in **3** nor in **4**. Thus, at low temperature where insufficient thermal energy limits the non-radiative channels, the lower $^3$MLCT energy of **2** (long component) is manifested in its red-shifted emission.

However, the emission of **4** in a 4 : 1 : 2 (v/v) EtOH–MeOH–$CH_3CN$ glass completely disappears above 122 K (see Fig. S12, S10), where also no emission is detectable in pure $CH_3CN$ at ambient temperature. Nevertheless, at 77 K **4** shows a strong emission centred at 521 nm for $\lambda_{ex}$ of 430 nm (see Fig. S5, page S6†). Thus, at 77 K the deactivation channel involving activated surface crossing from the $^3$MLCT state to the upper lying d → d excited level cannot enter into play due to insufficient thermal energy.[2b,5a,27] At this temperature the emission of **2** is red-shifted compared with **3** and **4** (*vide supra*). This leads to a significantly smaller luminescence lifetime of the $^3$MLCT state (long component) of **2** at 77 K than in **3** and **4** in accord with the energy gap law (see ESI, Table 1, page S14†).[5a,32] Obviously, the enhanced availability of medium-frequency ring-stretching vibrations in **4** due to its pronounced flexibility of the square-planar coordination seen in its crystal structure favours the non-radiative decay. Furthermore, the described blue shift of the emission of **4** indicates the higher energy of its $^3$MLCT state, making the d → d state more accessible.[5a,12a] Both effects together inhibit the emission of **4** above 122 K.

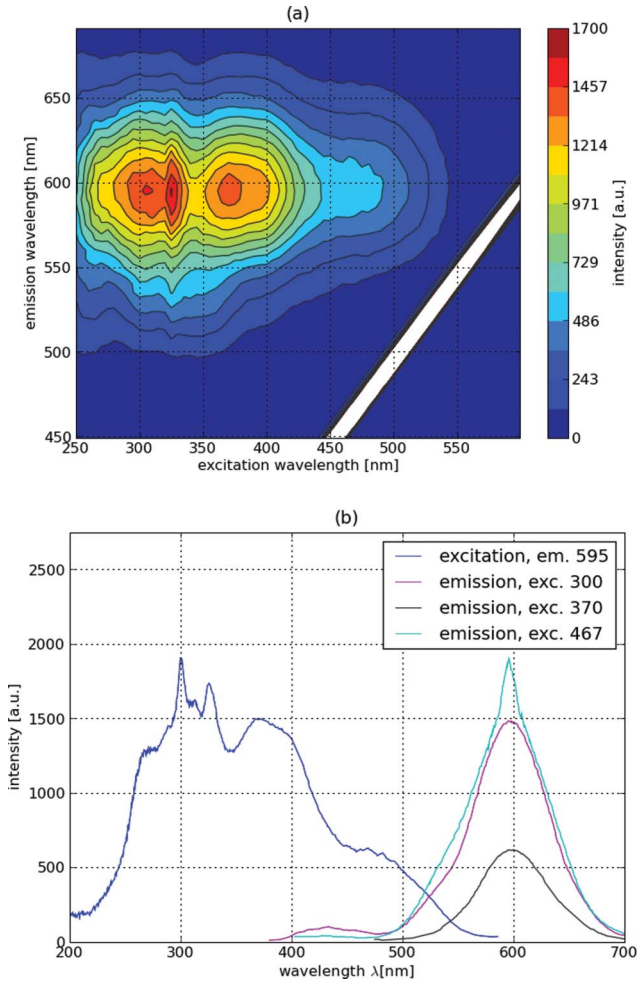


**Fig. 5** Contour plot of the combined absorption and luminescence spectra of **9** in $CH_3CN$ at 298 K (a) and excitation and emission spectra of **9** in $CH_3CN$ at 298 K (b).

The emissions from the novel *trans*-$[Ru(bpy)(CH_3CN)_2]^{2+}$ chromophore in **7** and **8** are clearly observable at 77 K (see Fig. S8 and S10, pages S7, S8†). They occur at 455 nm for $\lambda_{ex}$ of 270 nm in the case of **7** and at 480 nm for $\lambda_{ex}$ of 260 nm in the case of **8**. In order to improve the emissions 10 : 1 : 5 (v/v) EtOH/glycerol/$CH_3CN$ glasses were used. These emissions stem from the $^3$MLCT states, since they show the typical very long luminescence lifetimes of 5.5(6) μs (**7**) and 4.5(2) μs (**8**) at 77 K (see ESI, Table 1, page S14†).[2b,5a,12a] A pronounced blue shift is observed for these $^3$MLCT emissions compared with the corresponding transitions of **2–4**. The crystal structures of **7** and **8** clearly indicate that the stretching vibration modes of $CH_3CN$ are readily available. Therefore, for analogous reasons as in the case of **4** the $^3$MLCT emissions of **7** and **8** are only detectable at 77 K and immediately disappear during warming-up. The ambient temperature emissions of **7** and **8** stem from different states and are obscured by the $^3$MLCT emissions at 77 K. As in the case of **2** they could be attributed to the introduction of square-planar metal centres. For **7** this emission occurs at 385 nm for $\lambda_{ex}$ of 275 nm, where the pronounced excitation shoulder at 325 nm clearly belongs to the same emissive state (see Fig. S7, page S7†). **8** shows a comparable emission at 400 nm for $\lambda_{ex}$ of 290 nm (see Fig. S9, page S8†).

Fig. 5 shows the emission spectra of **9**. It is obvious that within a wide wavelength range, from about 200 to 600 nm, excitation occurs into the same emissive state. Independent from this wide excitation wavelength range always the same shape of the emission spectrum is obtained, clearly indicating that no impurities are involved. One should also note that the emission intensities exactly match the corresponding excitation intensities depending on the excitation wavelength. In **9** the combination of the *trans*-$[Ru(bpy)(CH_3CN)_2]^{2+}$ chromophore with the $[Os(bpy)_2]^{2+}$ chromophore leads to a system that possesses further stabilized MLCT excited states (predominantly triplet in character) relative to the homodimetallic analogs, as mentioned above.[30] Thus, independent of the excitation wavelength (300, 370 or 467 nm) emission is observed from the same state at 595 nm (see Fig. 5b). This means that light (solar) energy is efficiently transferred into a very distinct state. This could be important for water splitting experiments (*vide infra*). The typical blue shift is detected for this state at 77 K, the emission occurring at 565 nm independent of the excitation wavelength (300, 380 or 495 nm; see Fig. S11, page S9†).

### Excited state decay

The photophysical data related to the excited state decay of **2–4** and **7–9** are summarized in the ESI, Table 1, page S14.† At 77 K **2–4** and **7–9** show very long luminescence lifetimes ranging from 4.3(1) to 14.80(4) μs typical for $^3$MLCT states.[2b,5a,12a] The values of 4.4(3), 12.2(1), and 14.80(4) μs for **2–4**, respectively, are completely in line with the energy gap law,[5a,32] since the corresponding emission centres occur at 560, 529, and 521 nm. However, though a pronounced blue shift is observed for the $^3$MLCT emission centres of **7** and **8**, detected at 455 and 480 nm, respectively, the excited state lifetimes of 5.5(6) μs for **7** and 4.5(2) μs for **8** are significantly shorter than for **3** and **4**. Obviously, the introduction of the novel *trans*-$[Ru(bpy)(CH_3CN)_2]^{2+}$ chromophore into **7** and **8**, showing readily available stretching vibration modes of $CH_3CN$, dramatically reduces the luminescence lifetimes of **7** and **8** even at 77 K. Furthermore, in agreement with the emission spectrum of **9** at 77 K (see Fig. S11, page S9†) showing further stabilized MLCT states,[30] the simultaneous presence of the *trans*-$[Ru(bpy)(CH_3CN)_2]^{2+}$ and $[Os(bpy)_2]^{2+}$ chromophores in **9** also alters its luminescence lifetime of 4.3(1) μs, since this value is significantly larger than the corresponding parameter of 3.0(2) μs for the homodimetallic analog $[Os_2(dppcb)(bpy)_4]^{4+}$.[2b]

To the best of our knowledge there are only a few examples where the combination of $[Ru(bpy)_2]^{2+}$ chromophores with phosphines leads to long excited state lifetimes relating to the $^3$MLCT state of $[Ru(bpy)_2]^{2+}$ at ambient temperature.[2b,5a] For complexes of simple diphosphines like $[Ru(Me_2P(CH_2)_2PMe_2)(bpy)_2]^{2+}$ measurements of luminescence lifetimes at ambient temperature were not possible due to an estimated emission quantum yield ($\phi_r$) of ~ $10^{-6}$, which is at the limit of the detection capabilities.[12a] Thus, the obvious presence of "steric pressure" in **2** and **3** enhances their luminescence due to a reduction of the non-radiative decay and two further rare long excited state lifetimes at ambient temperature of 299(6) ns for **2** and of 261(10) ns for **3** were determined. A long-lived excited state at ambient temperature as in **2** or **3** is necessary for photochemical reactions occurring within a ns time scale.[24,33] The reactivity properties of comparable complexes have turned out to be quite extraordinary based on the accessibility of

 

long-lived excited states.[5b,34] Therefore, completely in line with these considerations the photochemical reactions of **2** and **3** leading to **7** and **8**, respectively, occur smoothly and could also be regarded as extraordinary, since chelating bpy ligands are replaced by the solvent molecules $CH_3CN$. The same is true for the photochemical reactivity of **5/6**, showing long-lived excited states at ambient temperature and hence also a clean photochemical reaction yielding **9**.[2b] As already mentioned, any emission disappears at ambient temperature in the case of **4** due to an enhanced non-radiative decay. Obviously, this non-radiative decay is fast enough to prevent also any distinctive photochemical reaction. The short lifetimes of 17.0(2) ns for **7** and 12.10(8) ns for **8** are attributed to different states. As for **2** with a short component of the emission of 6.4(5) ns at 77 K and 3.5(5) ns at 298 K (Table 1 in the ESI, page S14†), the presence of square-planar metal centres in **2**, **7**, and **8** could be responsible for these short lifetimes.

However, **9** shows the most interesting feature regarding its emission properties. Comparable to **5/6** also **9** is a combination of a Ru-centred "antenna" site with an Os-centred "trap" site.[2b,10] This means that light absorption at the "antenna" site is indirectly coupled to electron transfer to the "trap" site by the use of intervening energy transfer. The $^3$MLCT emission centres of **7**–**9** at 77 K clearly reveal what happens in **9**. They occur at 455 (**7**), 480 (**8**), and 565 (**9**) nm. Obviously, these emissions of **7** and **8** stem from their *trans*-$[Ru(bpy)(CH_3CN)_2]^{2+}$ chromophores. However, though this chromophore is also present in **9**, its emission centre is clearly related to its $[Os(bpy)_2]^{2+}$ chromophore.[2b,4] This means that within a wide excitation range (see Fig. S11, page S9†) energy is transferred to an Os-centred $^3$MLCT state, where typically and as in the case of **5/6** excitation at $Ru^{II}$ leading to $Os^{II}$* is independent of excitation wavelength.[2b,10] Also independent of excitation wavelength and temperature (*vide infra*), single exponentials completely fit the signals in all cases. Therefore, proof positive is given that the $Ru^{II}$ moiety in **9** acts as efficient "antenna" for visible light-driven energy transfer to the Os-centred "trap" site. A picosecond laser setup revealed that $Os^{II}$* was formed within the instrument response of the apparatus used (fwhm < 500 ps), resulting in $k_{en} \geq 2 \times 10^9$ s$^{-1}$ for the energy transfer.[2b,10] The value of $k_{en}$ indicates that like in **5/6** also in **9** the Dexter (exchange) transfer is favoured for which triplet–triplet transfer is allowed, since the MLCT excited states are largely triplet in character.[2b,10,19] This energy transfer mechanism requires overlap of the wavefunctions of the $Ru^{II}$ energy donor and the $Os^{II}$ energy acceptor. The Os···Ru distance in **9** is 7.396(1) Å, where it is well-known that for Os···Ru distances of 7 ± 2 Å through-space mechanisms of energy transfer come into play.[2b,10] In **9** energy transfer *via* the backbone can be neglected, since a region of saturated carbons disrupts significant electronic wave function mixing through the cyclobutane backbone "bridge".

Also at ambient temperature the luminescence lifetime of 297(4) ns for **9** (see Table 1 in the ESI, page S14†) is significantly larger than the corresponding parameter of 243(8) ns for the homodimetallic analog $[Os_2(dppcb)(bpy)_4]^{4+}$.[2b] As discussed above for 77 K the simultaneous presence of the *trans*-$[Ru(bpy)(CH_3CN)_2]^{2+}$ and $[Os(bpy)_2]^{2+}$ chromophores in **9** alters its luminescence lifetime due to a further stabilized Os-centred $^3$MLCT state, as indicated by its wavelengths of the emission centres at 77 and 298 K. Therefore, it seemed interesting to see, whether of not this "new" state is still capable of thermally activated surface crossing to the upper lying d → d excited level.[2b,5a,27] The Arrhenius plot between 100 and 298 K of ln $\tau$ *versus* 1000/T of **9** is shown in Fig. S13, page S10.† The highly activated decay process within the liquid range above about 265 K is characteristic of the $^3$MLCT → d → d crossover.[2b,5a,12a] The derived magnitude of the activation energy ($E_a$) for this process of 812 cm$^{-1}$ is completely in line with the estimate that an upper limit for $E_a$ is ~ 850 cm$^{-1}$ for the $RuP_2N_4$ phosphine complexes.[12a] The related value of $k'$ at 298 K of $2.74 \times 10^6$ s$^{-1}$ indicates that the d → d state is readily populated at this temperature in **9**. The same is true for **2** and **3**, where all Arrhenius-type parameters $E_a$, $k'$, and $A$ are summarized in Table 1 in the ESI, page S14.† The emission quantum yields ($\phi_r$) are also given in Table 1 in the ESI,† when possible. They represent very low values and show that at least in principle most of the incoming light (solar) energy could be used for different purposes like chemical storage for this class of compounds.[2b,5a]

The electron and energy transition from dimetallic complexes of Ruthenium and Osmium has been extensively explored. However, this is only true for $RuN_6$ and $OsN_6$ moieties. In the case of the $RuP_2N_4$ and $OsP_2N_4$ moieties reported in this work, a full description of the electron and energy transition from related dimetallic complexes is extremely rare.[4] Furthermore, the presence of a bis(bidentate) tetraphosphine containing a saturated backbone makes MLCT excited states involving the bridging ligand itself impossible.[35] Hence the photophysics and the photophysical reactivity of the compounds presented in this work are completely new due to the presence of $RuP_2N_4$ and $OsP_2N_4$ moieties.

## Conclusions

When the energy difference between $^3$MLCT and d → d state is lower than about 850 cm$^{-1}$, no emission can be observed at room temperature for complexes of the type $[Ru(monophosphine)_2(bpy)_2]^{2+}$ and $[Ru(diphosphine)(bpy)_2]^{2+}$.[12a] This common rule is also fulfilled by analogous compounds containing dppcb, where the species **1** and **4** are examples.[5a] However, the diastereoisomers *meso*-(ΔΛ/ΛΔ)- and *rac*-(ΔΔ/ΛΛ)-$[Ru_2(dppcb)(bpy)_4](PF_6)_4$ show luminescence at ambient temperature connected with a long luminescence lifetime of 794(20) ns in $CH_3CN$.[5a] Since for this class of compounds the d → d states are readily populated at ambient temperature, non-radiative decay of these d → d states is typically dominated by energy loss into a series of medium-frequency ring-stretching vibrations with energy spacings between 1000 and 1600 cm$^{-1}$.[24] However, the availability of these vibrations mainly depends on the steric requirements of the excited molecules. The single-crystal X-ray structures of *meso*-(ΔΛ/ΛΔ)- and *rac*-(ΔΔ/ΛΛ)-$[Ru_2(dppcb)(bpy)_4](PF_6)_4$,[5b] **2**, and **3** indicate high "steric pressure" and therefore the availability of these vibrations is reduced. It should be regarded as a surprise that the "steric pressure" in **2** and **3** is still high enough in order to induce long luminescence lifetimes at ambient temperature of 299(6) ns for **2** and 261(10) ns for **3** in $CH_3CN$, despite the presence of sterically less demanding square-planar metal centres. The photophysical parameters of **2** and **3** are comparable to the related properties of the parent species, $[Ru(bpy)_3]^{2+}$, being moderately luminescent, with an emission lifetime of about 1 μs in fluid solution at room temperature.[36]

Three clean photoreactions of **2**, **3**, and **5**/**6** are presented in this work, where the clean photoreaction of *meso*-(ΔΛ/ΛΔ)- and *rac*-(ΔΔ/ΛΛ)-$[Ru_2(dppcb)(bpy)_4](PF_6)_4$ has already been described.[5] In all four cases no photoreactions occur in non-coordinating solvents, whereas $CH_3CN$ as solvent leads to strongly coordinated $CH_3CN$ ligands in the photoproducts. In all four cases the photoproducts have been fully characterized, including single-crystal X-ray structure analyses.[5b] The X-ray structures reveal that *trans*-$[Ru(bpy)(CH_3CN)_2]^{2+}$ moieties are present in all photoproducts, indicating a rearrangement of the remaining, still coordinated bpy ligand (see *e.g.* Fig. 4). Furthermore, bpy is a bidentate ligand, changing to an $\eta^1$-coordination mode during ligand release, where finally one bpy molecule is replaced by two $CH_3CN$ molecules. It is well-known that "self-annealing" effects could also be present due to intramolecular chelate ring closure in intermediates containing $\eta^1$-coordinated bpy ligands.[12a] It seems likely that for a photoreaction like this, occurring step by step, the excited state lifetime must not be too short. Indeed, in all four cases the clean photoreactivity is connected with the unequivocal measurements of long luminescence lifetimes at ambient temperature.

These considerations have been further proved by the photophysical and photochemical properties of the compounds **1**, **4**, and $[Ru(cis\text{-dppen})(bpy)_2]^{2+}$, where *cis*-dppen is *cis*-1,2-bis(diphenylphosphino)ethene.[5] The former two complexes show no emissions at ambient temperature and no clean photoreactions occurred. The latter species shows analogous properties to a series of comparable compounds containing simple mono- and diphosphines.[12a] Again these complexes show no emission at ambient temperature and they are photochemically stable. A solution of $[Ru(cis\text{-dppen})(bpy)_2]^{2+}$ in $CH_3CN$ was irradiated under the same conditions as the species **2**, **3**, and **5**/**6**. After 14 d, $[Ru(cis\text{-dppen})(bpy)_2]^{2+}$ is still present as the main component (> 90%).[5b] Obviously, these compounds have no long-lived excited states at ambient temperature. Therefore, the time scale for a photoreaction occurring step by step is too short and the depopulation of the d → d state is too fast. It should be regarded as another surprise that the "steric pressure" in **2** and **3** is also high enough for clean photoreactivity.

An enormous advantage in the use of the compounds presented in this work for solar energy conversion purposes is the thermal and photochemical stability of the bridging moiety induced by the bis(bidentate) tetraphosphine dppcb. Thus *e.g.* the compounds *meso*-(ΔΛ/ΛΔ)- and *rac*-(ΔΔ/ΛΔ)-$[Ru_2(dppcb)(bpy)_4](PF_6)_4$ dissolved in DMF can be heated up to 150 °C under an atmosphere of air for one week without any significant decomposition. Furthermore, a saturated backbone like the cyclobutane ring in dppcb inhibits MLCT excitation involving the bridging ligand. This is a great advantage compared with the usual bipyridine-based bridging ligands, which are often prone to a degradation of the ligand system due to MLCT excitation and activated surface crossing to the upper lying d→d excited levels inducing bridging ligand loss photochemistry. In this context often the expression "spectator ligands" is used: phosphines are used in order to stabilize the catalysts, but are not sensitive to the catalytic turnovers.[37]

## Acknowledgements

This research was financially supported by the Fonds zur Förderung der wissenschaftlichen Forschung (FWF) and the Forschungsförderungsgesellschaft (FFG), Vienna, Austria, the Tiroler Wissenschaftsfonds, Innsbruck, Austria, and the companies Verbund AG and D. Swarovski & Co.

## Notes and references

1 (*a*) H. A. Meylemans, C.-F. Lei and N. H. Damrauer, *Inorg. Chem.*, 2008, **47**, 4060–4076; (*b*) O. S. Wenger, B. S. Leigh, R. M. Villahermosa, H. B. Gray and J. R. Winkler, *Science*, 2005, **307**(5706), 99–102; (*c*) J. H. Alstrum-Acevedo, M. K. Brennaman and T. J. Meyer, *Inorg. Chem.*, 2005, **44**, 6802–6827; (*d*) K. Kalyanasundaram and M. Grätzel, *Coord. Chem. Rev.*, 1998, **177**, 347–414.
2 (*a*) D. E. Polyanski, D. Cabelli, J. T. Muckerman, T. Fukushima, K. Tanaka and E. Fujita, *Inorg. Chem.*, 2008, **47**, 3958–3968; (*b*) R. Gutmann, S. Eller, M. Fessler, W. E. van der Veer, A. Dumfort, H. Kopacka, T. Müller and P. Brüggeller, *Inorg. Chem. Commun.*, 2007, **10**, 1510–1514.
3 S. Canaguier, V. Artero and M. Fontecave, *Dalton Trans.*, 2008, 315–325.
4 (*a*) E. Zahavy and M. A. Fox, *Chem.–Eur. J.*, 1998, **4**, 1647–1652; (*b*) P.-W. Wang and M. A. Fox, *Inorg. Chem.*, 1995, **34**, 36–41.
5 (*a*) R. Gutmann, G. Czermak, A. Dumfort, W. E. van der Veer, B. Hong, H. Kopacka, K.-H. Ongania, T. Bechtold and P. Brüggeller, *Inorg. Chem. Commun.*, 2005, **8**, 319–322; (*b*) R. Haid, R. Gutmann, T. Stampfl, C. Langes, G. Czermak, H. Kopacka, K.-H. Ongania and P. Brüggeller, *Inorg. Chem.*, 2001, **40**, 7099–7104.
6 W. Oberhauser, C. Bachmann, T. Stampfl, R. Haid, C. Langes, H. Kopacka, A. Rieder and P. Brüggeller, *Inorg. Chim. Acta*, 1999, **290**, 167–179.
7 (*a*) M. Fessler, S. Eller, C. Bachmann, R. Gutmann, B. Trettenbrein, H. Kopacka, T. Mueller and P. Brueggeller, *Dalton Trans.*, 2009, 1383–1395; (*b*) C. Bachmann, R. Gutmann, G. Czermak, A. Dumfort, S. Eller, M. Fessler, H. Kopacka, K.-H. Ongania and P. Brüggeller, *Eur. J. Inorg. Chem.*, 2007, 3227–3239.
8 W. Oberhauser, C. Bachmann, T. Stampfl, R. Haid, C. Langes, A. Rieder and P. Brüggeller, *Polyhedron*, 1998, **17**, 3211–3220.
9 (*a*) J. J. Concepcion, J. W. Jurss, M. K. Brennaman, P. G. Hoertz, A. O. T. Patrocinio, N. Y. M. Iha, J. L. Templeton and T. J. Meyer, *Acc. Chem. Res.*, 2009, **42**, 1954–1965; (*b*) V. Balzani, A. Credi and M. Venturi, *ChemSusChem*, 2008, **1**, 26–58; (*c*) S. Swavey, Z. Fang and K. J. Brewer, *Inorg. Chem.*, 2002, **41**, 2598–2607.
10 C. N. Fleming, L. M. Dupray, J. M. Papanikolas and T. J. Meyer, *J. Phys. Chem. A*, 2002, **106**, 2328–2334 .
11 Y. Na, M. Wang, J. Pan, P. Zhang, B. Åkermark and L. Sun, *Inorg. Chem.*, 2008, **47**, 2805–2810.
12 (*a*) J. V. Caspar and T. J. Meyer, *Inorg. Chem.*, 1983, **22**, 2444–2453; (*b*) B. P. Sullivan, D. J. Salmon and T. J. Meyer, *Inorg. Chem.*, 1978, **17**, 3334–3341.
13 J. V. Caspar and T. J. Meyer, *J. Am. Chem. Soc.*, 1983, **105**, 5583–5590.
14 P. A. Anderson, F. R. Keene, T. J. Meyer, J. A. Moss, G. F. Strouse and J. A. Treadway, *J. Chem. Soc., Dalton Trans.*, 2002, 3820–3831.
15 (*a*) J.-P. Collin, D. Jouvenot, M. Koizumi and J.-P. Sauvage, *Inorg. Chem.*, 2005, **44**, 4693–4698; (*b*) T. Kojima, T. Sakamoto and Y. Matsuda, *Inorg. Chem.*, 2004, **43**, 2243–2245.
16 Z. Otwinowski and W. Minor, in *Methods in Enzymology*, *Macromolecular Crystallography, Part A*, ed. C. W. Carter, Jr. and R. M. Sweet, Academic Press, New York, 1997, vol. 276, pp. 307–326.
17 G. M. Sheldrick, *Acta Crystallogr., Sect. A: Found. Crystallogr.*, 1990, **46**, 467–473.
18 G. M. Sheldrick, *SHELXL-97, Program for refinement of crystal structures*, University of Göttingen, Germany, 1997.
19 L. De Cola and P. Belser, *Coord. Chem. Rev.*, 1998, **177**, 301–346.
20 (*a*) T. Stampfl, R. Gutmann, G. Czermak, C. Langes, A. Dumfort, H. Kopacka, K.-H. Ongania and P. Brüggeller, *Dalton Trans.*, 2003, 3425–3435; (*b*) H. C. E. McFarlane and W. McFarlane, *Polyhedron*, 1999, **18**, 2117–2127.
21 W. Oberhauser, T. Stampfl, C. Bachmann, R. Haid, C. Langes, H. Kopacka, K.-H. Ongania and P. Brüggeller, *Polyhedron*, 2000, **19**, 913–923.
22 C. Bianchini, L. Gonsalvi, W. Oberhauser, D. Sémeril, P. Brüggeller and R. Gutmann, *Dalton Trans.*, 2003, 3869–3875.
23 H. S. Chow, E. C. Constable, C. E. Housecroft, M. Neuburger and S. Schaffner, *Dalton Trans.*, 2006, 2881–2890.

 

24 J. A. Treadway, B. Loeb, R. Lopez, P. A. Anderson, F. R. Keene and T. J. Meyer, *Inorg. Chem.*, 1996, **35**, 2242–2246.
25 H. A. Mayer and W. C. Kaska,, *Chem. Rev.*, 1994, **94**, 1239–1272.
26 S. A. McFarland and N. S. Finney, *Chem. Commun.*, 2003, 388–389.
27 F. Barigelletti, L. De Cola, V. Balzani, R. Hage, J. G. Haasnot, J. Reedijk and J. G. Vos, *Inorg. Chem.*, 1991, **30**, 641–645.
28 (*a*) A. Harriman, F. M. Romero, R. Ziessel and A. C. Benniston, *J. Phys. Chem. A*, 1999, **103**, 5399–5408; (*b*) J. Schneider, P. Du, P. Jarosz, T. Lazarides, X. Wang, W. W. Brennessel and R. Eisenberg, *Inorg. Chem.*, 2009, **48**, 4306–4316.
29 L. Moriggi, A. Aebischer, C. Cannizzo, A. Sour, A. Borel, J.-C. G. Bünzli and L. Helm, *Dalton Trans.*, 2009, 2088–2095.
30 S. Zhao, S. M. Arachchige, C. Slebodnick and K. J. Brewer, *Inorg. Chem.*, 2008, **47**, 6144–6152.
31 (*a*) X.-y. Wang, A. Del Guerzo and R. H. Schmehl, *J. Photochem. Photobiol., C*, 2004, **5**, 55–77; (*b*) M. L. Myrick and M. K. De Armond, *J. Phys. Chem.*, 1989, **93**, 7099–7107.
32 (*a*) M. W. Perkovic, *Inorg. Chem.*, 2000, **39**, 4962–4968; (*b*) N. J. Turro, *Modern Molecular Photochemistry*, University Science Books, Sausalito, California, 1991, p. 183.
33 G. Albano, P. Belser and C. Daul, *Inorg. Chem.*, 2001, **40**, 1408–1413.
34 T. J. Meyer and M. H. V. Huynh, *Inorg. Chem.*, 2003, **42**, 8140–8160.
35 C. Chiorboli, M. A. J. Rodgers and F. Scandola, *J. Am. Chem. Soc.*, 2003, **125**, 483–491.
36 S. A. McFarland, D. Magde and N. S. Finney, *Inorg. Chem.*, 2005, **44**, 4066–4076.
37 It was possible to unequivocally observe oxidative quenching of the $^3$MLCT states related to the $[Os(bpy)_2]^{2+}$ chromophores in $[Os(bpy)_2(dppcb)MCl_2](SbF_6)_2$ (M = Pt, Pd, Ni) in their Arrhenius plots.[38] This means that electron transfer occurs by the use of intervening energy transfer and a highly reactive M(I) species is formed in an one-electron step.[39] In the presence of a sacrificial electron donor this step could be repeated and in two subsequent one-electron steps M(0) could be generated. However, analogous to Co(I), M(0) (M = Pt, Pd, Ni) is not stable in water and M(II) hydride intermediates are usually produced.[39] These hydrides react with $H^+$ to give $H_2$, thus regenerating the initial M(II) compound. Therefore, in order to stabilize the M(0) state by further chelating bpy ligands the complexes $[Ru(bpy)_2(dppcb)M(bpy)](PF_6)_4$ (M = Pt, Pd) were prepared, showing water solubility.[4,38] Furthermore, four different systems have been studied by our working group with regard to the photogeneration of hydrogen from water. They consist of the complexes $[Ru(bpy)_2(dppcb)M(bpy)](PF_6)_4$ (M = Pt, Pd) and $[Os(bpy)_2(dppcb)M(bpy)](PF_6)_4$ (M = Pt, Pd), respectively, in 1 : 1 (v/v) $H_2O$–$CH_3CN$, containing ascorbic acid as sacrificial electron donor. Interestingly, both $Pt^{II}$ species are nearly inactive, showing a hydrogen production at the detection limit. However, both $Pd^{II}$ compounds give detectable amounts of hydrogen. Thus, for the $Ru^{II}$–$Pd^{II}$ complex a TON of about 1 was observed after 12 h of photolysis and for the $Os^{II}$–$Pd^{II}$ species a TON of 2.5 resulted after 2 h of photolysis. This means that the latter productivity is comparable to the systems of R. Eisenberg[28b] and L. Sun[11] and as in their cases should be regarded as an illustration of the concept. Since in the $Os^{II}$ complex the deactivation channel involving activated surface crossing to the upper lying d → d excited levels cannot enter into play,[2b,27] only a photophysical reactivity is present, leading to the production of hydrogen. However, the $Ru^{II}$ species could show a bpy ligand loss photochemistry comparable to compound **3**. In this case the photochemical reactivity of $[Ru(bpy)_2(dppcb)Pd(bpy)](PF_6)_4$ could be detrimental to its photophysical reactivity, reducing the amount of hydrogen produced. Possible dark reactions and/or $H_2$ production from *in situ* formed colloidal particles during photolysis have been carefully ruled out.[39] In this process, light (solar) energy is stored in the bond rearrangement of $H_2O$ to $H_2$ and $O_2$.[9b,40] Our future studies will focus on the improvement of the TON for $H_2$ production. It is by no means easy to replace noble metals like platinum in **2** or palladium in **3** with nickel in **4**, since the photophysical and photochemical properties of **4** are completely different from **2** or **3**. An "ideal" photocatalyst should contain *e.g.* a copper(I) chromophore instead of ruthenium(II) or osmium(II) and *e.g.* a nickel(II) or Fe2S2 catalyst for $H_2$ evolution. However, this problem can only be solved step by step.
38 P. Brüggeller, S. Eller and B. Trettenbrein, unpublished results.
39 P. Du, J. Schneider, G. Luo, W. W. Brennessel and R. Eisenberg, *Inorg. Chem.*, 2009, **48**, 4952–4962.
40 D. G. Nocera, *Chem. Soc. Rev.*, 2009, **38**, 13–15.